ELECTRIC POWER RESEARCH INSTITUTE

2013 TECHNICAL REPORT

BWRVIP-275NP: BWR Vessel and Internals Project

Testing and Evaluation of the Susquehanna Unit 1 120° Capsule

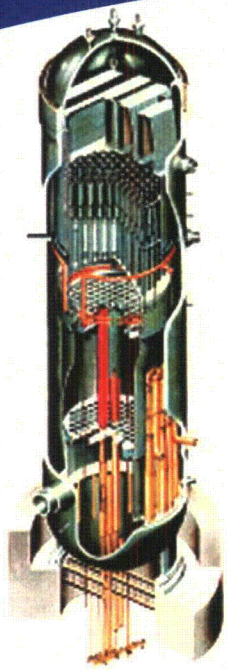

PREPARED UNDER THE NUCLEAR QA PROGRAM

BWRVIP-275NP: BWR Vessel and Internals Project

Testing and Evaluation of the Susquehanna Unit 1 120° Capsule

All or a portion of the requirements of the EPRI Nuclear Quality Assurance Program apply to this product.

YES NO

EPRI Project Manager
R. Carter

ELECTRIC POWER RESEARCH INSTITUTE

3420 Hillview Avenue
Palo Alto, CA 94304-1338
USA

PO Box 10412
Palo Alto, CA 94303-0813
USA

800.313.3774
650.855.2121

askepri@epri.com

www.epri.com

3002000685
Final Report, October 2013

DISCLAIMER OF WARRANTIES AND LIMITATION OF LIABILITIES

THE FOLLOWING ORGANIZATIONS PREPARED THIS REPORT:

Electric Power Research Institute (EPRI)

MP Machinery & Testing, LLC

TransWare Enterprises Inc.

THE TECHNICAL CONTENTS OF THIS PRODUCT WERE PREPARED IN ACCORDANCE WITH THE EPRI QUALITY PROGRAM MANUAL THAT FULFILLS THE REQUIREMENTS OF 10 CFR 50 APPENDIX B. THIS PRODUCT IS SUBJECT TO THE REQUIREMENTS OF 10 CFR PART 21. CERTIFICATION OF CONFORMANCE CAN BE OBTAINED FROM EPRI.

NOTE

For further information about EPRI, call the EPRI Customer Assistance Center at 800.313.3774 or e-mail askepri@epri.com.

Acknowledgments

The following organizations prepared this report:

Electric Power Research Institute (EPRI)
3420 Hillview Ave.
Palo Alto, CA 94304

Principal Investigators
T. Hardin
K. Wolfe

MP Machinery & Testing, LLC
2161 Sandy Drive
State College, PA 16803

Principal Investigator
M. P. Manahan, Sr.

TransWare Enterprises Inc.
1565 Mediterranean Drive
Sycamore, IL 60178

Principal Investigator
E. Jones

This report describes research sponsored by EPRI and its Boiling Water Reactor Vessel and Internals Project (BWRVIP) participating members.

This publication is a corporate document that should be cited in the literature in the following manner:

BWRVIP-275NP: BWR Vessel and Internals Project: Testing and Evaluation of the Susquehanna Unit 1 120° Capsule.
EPRI, Palo Alto, CA: 2013.
3002000685.

Product Description

In the late 1990s, a Boiling Water Reactor Vessel and Internals Project (BWRVIP) Integrated Surveillance Program (ISP) was developed to improve the surveillance of the U.S. BWR fleet. This report describes testing and evaluation of the Susquehanna Unit 1 120° capsule. These results will be used to monitor embrittlement as part of the BWRVIP ISP.

Background

The BWRVIP ISP represents a major enhancement to the process of monitoring embrittlement for the U.S. fleet of BWRs. The ISP optimizes surveillance capsule tests while, at the same time, maximizing the quantity and quality of data, thus resulting in a more cost-effective program. The BWRVIP ISP provides more representative data that can be used to assess embrittlement in reactor pressure vessel beltline materials and improve trend curves in the BWR range of irradiation conditions.

Objectives

Neutron irradiation exposure reduces the toughness of reactor vessel steel plates, welds, and forgings. The objectives of this project were twofold:

- To document the results of neutron dosimetry and Charpy V-notch ductility tests for the surveillance materials (plate heat C2433-1 and weld heat 402K9171, 411L3071) in the Susquehanna Unit 1 120° capsule
- To compare the results with the embrittlement trend prediction of the U.S. Nuclear Regulatory Commission (U.S. NRC) Regulatory Guide 1.99, Revision 2

Approach

The Susquehanna Unit 1 120° capsule had been irradiated in the reactor since plant startup. The surveillance capsule contained flux wires for neutron flux monitoring, Charpy V-notch impact test specimens, and tensile specimens. The project team removed the capsule from the reactor in 2012 and transported it to facilities for testing and evaluation. The team used dosimetry to gather information about the neutron fluence accrual of specimens from the capsule. They then performed a neutron transport calculation in accordance with Regulatory Guide 1.190 and compared it to the results from the dosimetry. Testing of Charpy V-notch specimens was performed according to the standards of ASTM International.

Results

The report includes capsule neutron exposure and Charpy V-notch test results for Susquehanna Unit 1 surveillance plate heat C2433-1 and surveillance weld 402K9171, 411L3071. The project compared irradiated Charpy data to unirradiated data in order to determine the shifts in Charpy index temperatures for the surveillance plate and weld materials due to irradiation. For the surveillance plate, the measured shift is less than the predicted shift + margin using Regulatory Guide 1.99, Revision 2. However, for the weld, the measured shift is about 2.5 times greater than the predicted shift + margin. Researchers also measured flux wires, determined fluence for the 120° capsule, and calculated a revised fluence for the previously tested 30° capsule.

Applications, Value, and Use

Results of this work will be used in the BWRVIP ISP, which integrates individual BWR surveillance programs into a single program. The ISP provides data of high quality to monitor BWR vessel embrittlement. The ISP results in significant cost savings to the BWR fleet and provides more accurate monitoring of embrittlement in BWR vessels.

Keywords

BWR
Charpy testing
Mechanical properties
Radiation embrittlement
Reactor pressure vessel integrity
Reactor vessel surveillance program

Table of Contents

List of Figures

List of Tables

Section 1: Introduction

Test coupons of reactor vessel ferritic beltline materials are irradiated in reactor surveillance capsules to facilitate evaluation of vessel fracture toughness in vessel integrity evaluations. The key values that characterize fracture toughness are the reference temperature of nil-ductility transition (RT_{NDT}) and the upper shelf energy (USE). These are defined in 10CFR50 Appendix G [1] and in Appendix G of the ASME Boiler and Pressure Vessel Code, Section XI [2]. Appendix H of 10CFR50 [1] and ASTM E185-82 [3] establish the methods to be used for testing of surveillance capsule materials.

In the late 1990s the BWR Vessel and Internals Project (BWRVIP) initiated the BWRVIP Integrated Surveillance Program (ISP) [4], and the BWRVIP assumed responsibility for testing and evaluation of ISP capsules. The surveillance plate and weld from Susquehanna Steam Electric Station, Unit 1 (hereinafter, Susquehanna 1) were designated as "ISP representative surveillance materials" to be tested by the ISP according to an approved capsule withdrawal and test schedule.

This report addresses the withdrawal and test of the Susquehanna 1 120° surveillance capsule. The capsule contained flux wires for neutron flux monitoring, Charpy V-notch impact test specimens, and tensile specimens. The capsule was irradiated for 17 cycles of operation before it was removed in April 2012 and shipped to MP Machinery & Testing, LLC for opening and testing of the Charpy V-notch surveillance specimens. Evaluation of the fluence environment was conducted by TransWare Enterprises, Inc. Final evaluation of the Charpy test data and irradiated material properties and compilation of this report were performed by EPRI. The Charpy V-notch surveillance materials were tested per ASTM E185-82, and the information and the associated evaluations provided in this report have been performed in accordance with the requirements of 10CFR50 Appendix B [5].

This report compares the irradiated material properties of surveillance plate heat C2433-1 and surveillance weld 402K9171, 411L3071 to their baseline (e.g., unirradiated) properties. The observed embrittlement (as characterized by the shift in the Charpy energy curve 30 ft-lb (41J) index temperature, or ΔT_{30}) is compared to that predicted by U.S. Nuclear Regulatory Commission (U.S. NRC) Regulatory Guide 1.99, Rev. 2 [6]. Other BWRVIP ISP reports will integrate the results from the 120° capsule with the results from the 30° capsule (tested in 1993) for a broader characterization of embrittlement behavior.

1.1 Implementation Requirements

The results documented in this report will be utilized by the BWRVIP ISP and by individual utilities to demonstrate compliance with 10CFR50, Appendix H, Reactor Vessel Material Surveillance Program Requirements. Therefore, the implementation requirements of 10CFR50, Appendix H govern and the implementation requirements of Nuclear Energy Institute (NEI) 03-08, Guideline for the Management of Materials Issues [7], are not applicable.

Section 2: Materials and Test Specimen Description

The General Electric (GE) designed Susquehanna Unit 1 120° surveillance capsule was removed from the plant for analysis and testing during the April, 2012 refueling outage. The capsule was a GE standard single basket design and contained a total of two Charpy packets and four tensile tubes. Within each Charpy packet were a total of 12 Charpy V-notch specimens and three high purity dosimetry wires. Each of the tensile tubes contained two tensile specimens. The 120° capsule is an original plant capsule, and had been irradiated in the plant since initial startup. This is the second surveillance capsule to be removed from Susquehanna 1 and tested. The 30° capsule was removed from the plant in early 1992 and was tested by GE [8].

2.1 Dosimeters

The dosimetry wires were located along the ends of the Charpy specimens during irradiation. Each of the two Charpy packets contained one high purity iron, copper, and nickel wire for fluence determination. Further details on the exact wire locations during the irradiation are provided in the capsule opening discussion given in Section 2.3. A detailed discussion of the radiometric analysis of the capsule dosimetry wires is provided in Appendix A.

2.2 Test Materials

The 120° capsule Charpy V-notch and tensile specimen inventory, material descriptions, unirradiated (baseline) Charpy impact data, and previously measured capsule data are summarized in this section of the report. Fabrication history of the vessel and test specimens, including heat treatment, was reported in [8].

2.2.1 Capsule Loading Inventory

The Susquehanna 1 120° surveillance capsule inventory is provided in Table 2-1. All of the capsule specimens, which include tensile specimens, Charpy specimens, and dosimeters, were recovered from the capsule basket. Testing was performed on the 24 Charpy specimens, and the dosimetry wires were counted and weighed to determine specific activities. All eight of the tensile specimens (three base, three weld, and two HAZ) remain untested and are being held in

reserve for future testing since there is no near-term use for the tensile data. The technical advantage of storing the tensile specimens untested is that there will be options in the future for how these specimens will be used to obtain useful data. For example, the tensile specimen geometry is conducive to fabrication of subsize Charpy as well as miniaturized Charpy V-notch specimens. Further, research is currently underway to develop testing methods which will enable the determination of plane-strain fracture toughness data from Charpy-sized specimens. With these new technologies in view, there may be a need in the future for static and/or dynamic tensile data for use in the calculation of fracture toughness from experimental data obtained from Charpy specimens. Therefore, all of the tensile specimens have been placed into the archive storage so that they can be tested when necessary in the future. Similarly, the broken Charpy specimen halves have been added to long-term archive storage for future use in miniature mechanical behavior specimen testing, chemistry analysis, and microstructural studies.

As indicated in Table 2-1, there were a total of two Charpy packets in the capsule, and each contained three dosimetry wires (one Fe wire, one Cu wire, and one Ni wire) and 12 Charpy specimens. Charpy packet G4 was found to contain all of the base metal test specimens as well as 4 weld specimens. Charpy packet G5 contained the remaining four weld specimens along with all of the HAZ specimens. A drawing of the Charpy test specimen is shown in Figure 2-1 for reference. A photograph of the capsule and a schematic showing the position of the specimens within the capsule are shown in Figures 2-2 and 2-3, respectively.

Table 2-1
Susquehanna Unit 1 120° Surveillance Capsule Specimen Inventory

Susquehanna Unit 1 120° Surveillance Capsule Contents and Locations[1]							
Charpy Packet No.[2]	**Number of Charpy Specimens**			**Number of Flux Wires**			**Relative Vertical Position**
	Base	Weld	HAZ	Fe	Cu	Ni	
G5	0	4	8	1	1	1	Highest Charpy Packet in Basket
G4	8	4	0	1	1	1	Lowest Charpy Packet in basket

[1] The surveillance program includes tensile specimens, but the tensile specimens were not tested. All eight tensile specimens for this capsule were located at the lowest axial positions below Charpy packet G4.

[2] The packet numbers in this table are organized by axial position in the capsule with packet G4 at the lowest elevation in the reactor and packet G5 at the highest.

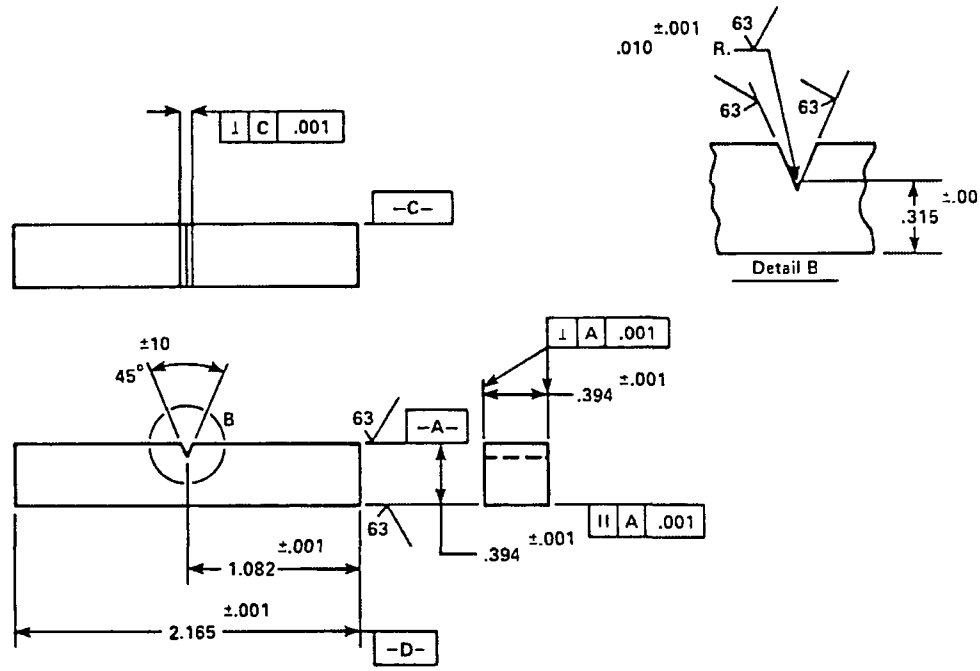

Figure 2-1
Drawing Showing the Charpy Test Specimen Geometry

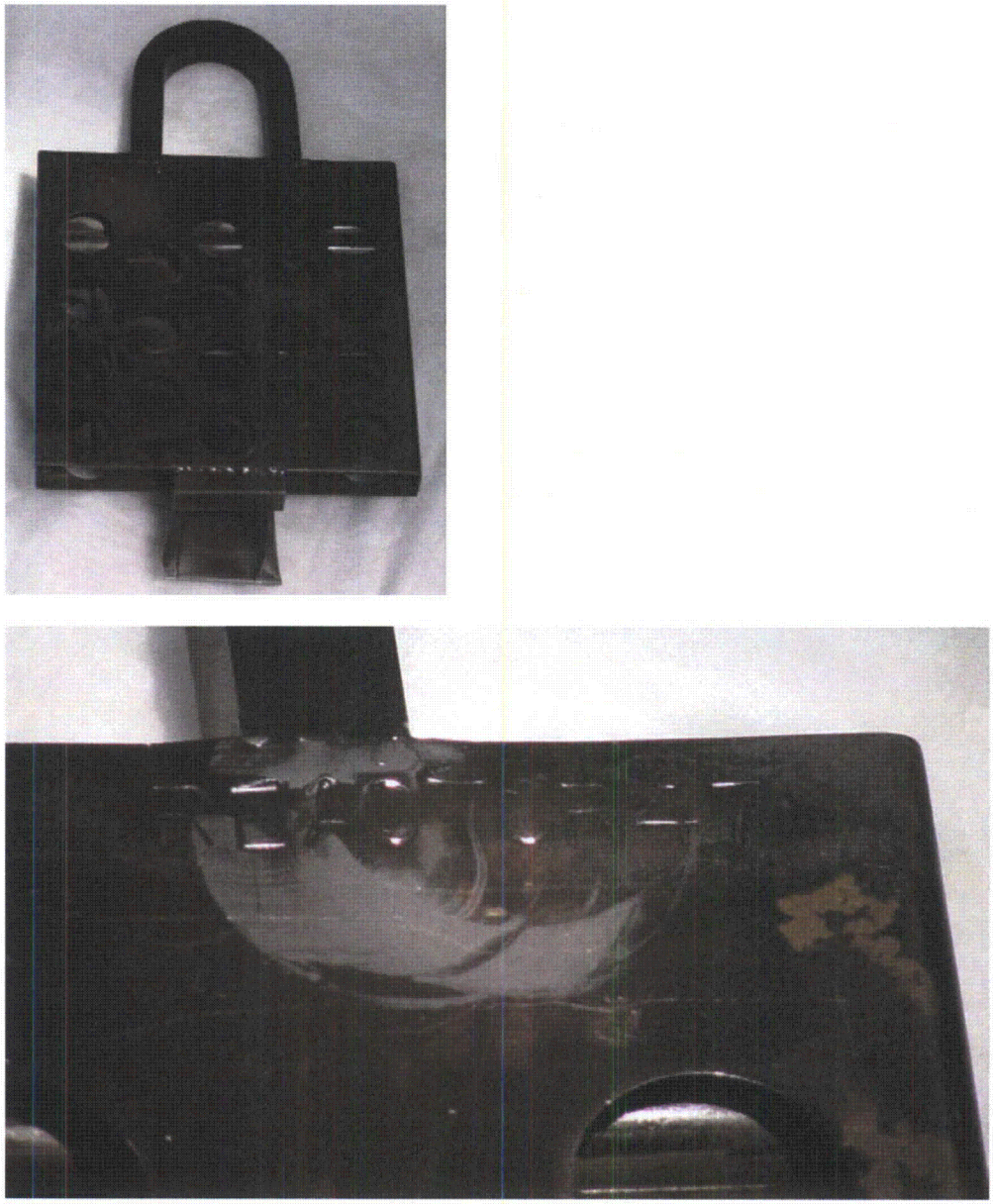

Figure 2-2
Photograph of 120° Capsule for Susquehanna Unit 1

The Upper Photograph Shows the Outer Basket, and the Lower Photograph Shows the Correct Reactor Number Engraved on the Basket. In the Two Photographs, the Side which Faced the Pressure Vessel in the Plant is Facing Up

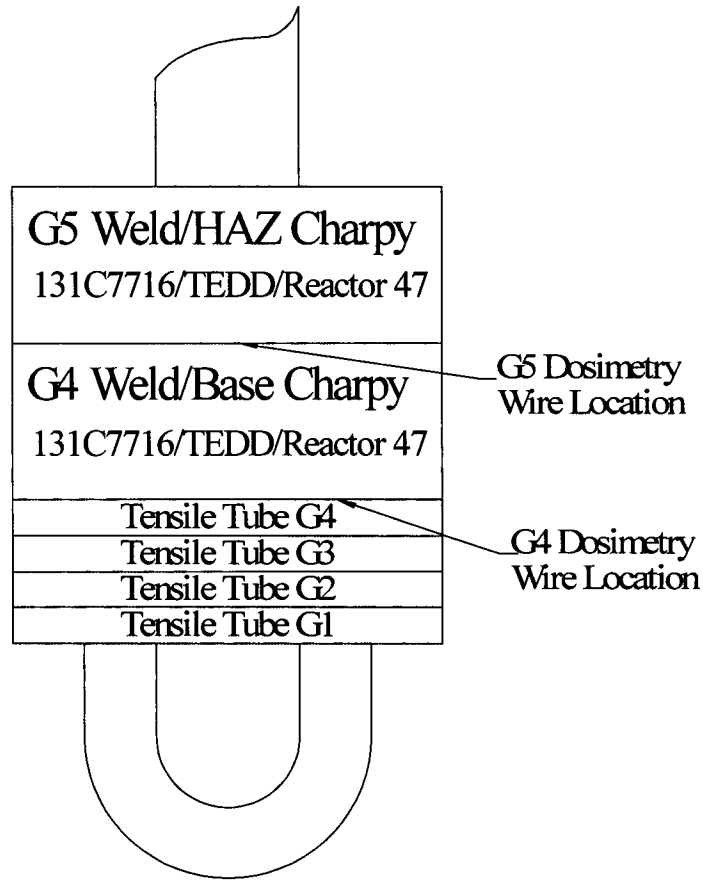

Figure 2-3
Schematic Drawing Showing the Locations of Test Specimens in the Susquehanna 1 120° Surveillance Capsule

2.2.2 Material Description

The surveillance base metal specimens were machined from plate heat number C2433-1 in the longitudinal orientation (LT). Unirradiated baseline data are available for this material, and for the weld and HAZ materials as well. All of the base metal specimens were stamped on the ends, with the markings P1 on one end and 47 on the other end, as assigned by GE. As each specimen was removed from the capsule, it was assigned a sequential numbering to establish a unique identity and to document the position of each specimen in the packet.

The weld and HAZ Charpy surveillance specimens were made by welding together two pieces of the surveillance test plate heat C2433-1. Reference 8 reported that the vessel fabricator's welding records (Chicago Bridge & Iron) show that the surveillance weld is a shielded metal arc weld with one or both of two heats designated as 411L3071/L311A27AF and 402K9171/K315A27AE (heat/lot). In this report, the surveillance weld is identified by using the heat numbers, as "402K9171, 411L3071".

2.2.3 Chemical Composition

Table 2-2 details the best estimate average chemistry values for plate heat C2433-1 surveillance material. Chemical compositions are presented in weight percent. If there are multiple measurements on a single specimen, those are first averaged to yield a single value for that specimen, and then the different specimens are averaged to determine the heat best estimate.

Table 2-2
Best Estimate Chemistry of Available Data Sets for Plate Heat C2433-1

Cu (wt%)	Ni (wt%)	P (wt%)	S (wt%)	Si (wt%)	Specimen ID	Source
0.09	0.62	0.009	—	0.12	Tensile P1-47 (RT)	Reference 8
0.09	0.59	0.009	—	0.18	Tensile P1-47 (550 deg F)	
0.09	0.605	0.009	—	0.15	Average P1-47	
0.10	0.63	0.009	0.015	0.23	Baseline plate (CMTR)	Reference 8
0.10	0.62	0.009	0.015	0.19	←Best Estimate Average	

Table 2-3 details the best estimate average chemistry values for weld heat 402K9171, 411L3071 surveillance material. Chemical compositions are presented in weight percent. If there are multiple measurements on a single specimen, those are first averaged to yield a single value for that specimen, and then the different specimens are averaged to determine the heat best estimate.

Table 2-3
Best Estimate Chemistry of Available Data Sets for Weld Heat 402K9171, 411L3071

Cu (wt%)	Ni (wt%)	P (wt%)	S (wt%)	Si (wt%)	Specimen ID	Source
0.02	0.94	0.013	—	0.38[1]	Tensile P2-47(RT)	Reference 8
0.02	0.95	0.011	—	0.37[1]	Tensile P2-47 (550 deg F)	
0.02	0.945	0.012	—	0.375	Average P2-47	
0.02	0.95	0.012	—	0.38[1]	←Best Estimate Average	

Note:

1. Results may be low according to reporting documents [8].

2.2.4 CVN Baseline Properties

As noted above, the Susquehanna 1 surveillance plate Charpy specimens are longitudinal (LT) specimens. Table 2-4 provides the unirradiated (baseline)

Charpy test data for the C2433-1 surveillance plate material and Table 2-5 provides the unirradiated data for the weld [8].

Table 2-4
Unirradiated Charpy V-Notch Impact Test Results for Surveillance Base Metal Specimens (Heat C2433-1) from the Susquehanna 1 Surveillance Program

Base Unirradiated							
Specimen ID	Test Temperature		Impact Energy		Lateral Expansion		Percent Shear (%)
	°F	(°C)	ft-lb	(J)	mils	(mm)	
P1-47	-100.0	(-73.3)	3.00	(4.07)	4.5	(0.11)	6
P1-47	-60.0	(-51.1)	6.00	(8.13)	2.5	(0.06)	5
P1-47	-20.0	(-28.9)	14.00	(18.98)	17.0	(0.43)	11
P1-47	0.0	(-17.8)	20.00	(27.12)	23.0	(0.58)	31
P1-47	20.0	(-6.7)	31.50	(42.71)	35.0	(0.89)	30
P1-47	20.0	(-6.7)	60.00	(81.35)	45.0	(1.14)	37
P1-47	30.0	(-1.1)	36.50	(49.49)	31.0	(0.79)	28
P1-47	60.0	(15.6)	73.50	(99.65)	58.5	(1.49)	50
P1-47	100.0	(37.8)	101.00	(136.94)	80.5	(2.04)	80
P1-47	150.0	(65.6)	120.00	(162.70)	79.0	(2.01)	100
P1-47	200.0	(93.3)	133.00	(180.32)	85.0	(2.16)	100
P1-47	300.0	(148.9)	138.00	(187.10)	83.5	(2.12)	100

Table 2-5
Unirradiated Charpy V-Notch Impact Test Results for Surveillance Weld Metal Specimens (Heats 402K9171, 411L3071) from the Susquehanna 1 Surveillance Program

Weld Unirradiated							
Specimen ID	Test Temperature		Impact Energy		Lateral Expansion		Percent Shear (%)
	°F	(°C)	ft-lb	(J)	mils	(mm)	
P2-47	-100.0	(-73.3)	3.50	(4.75)	8.0	(0.20)	8
P2-47	-80.0	(-62.2)	14.00	(18.98)	8.5	(0.22)	18
P2-47	-60.0	(-51.1)	42.50	(57.62)	28.5	(0.72)	29
P2-47	-60.0	(-51.1)	18.00	(24.40)	16.0	(0.41)	24
P2-47	-40.0	(-40.0)	11.00	(14.91)	7.5	(0.19)	27
P2-47	-20.0	(-28.9)	52.00	(70.50)	45.0	(1.14)	41
P2-47	20.0	(-6.7)	64.50	(87.45)	48.5	(1.23)	56
P2-47	60.0	(15.6)	68.00	(92.19)	56.0	(1.42)	72
P2-47	100.0	(37.8)	90.00	(122.02)	75.0	(1.91)	89
P2-47	150.0	(65.6)	109.00	(147.78)	83.5	(2.12)	99
P2-47	200.0	(93.3)	114.00	(154.56)	87.5	(2.22)	100
P2-47	300.0	(148.9)	100.00	(135.58)	90.0	(2.29)	100

The baseline test data were fit to a hyperbolic tangent curve using the computer program CVGRAPH [9]. Figures 2-4 and 2-5 show the fitted Charpy energy data curves for the unirradiated plate and weld, respectively. Table 2-6 summarizes the baseline (unirradiated) Charpy V-notch properties (index temperatures) of plate heat C2433-1 and weld heat 402K9171, 411L3071. In this table and throughout this report, T_{30} is the 30 ft-lb (41 J) transition temperature; T_{50} is the 50 ft-lb (68 J) transition temperature; T_{35mil} is the 35 mil (0.89 mm) lateral expansion temperature; and USE is the average energy absorption at full shear fracture appearance.

Table 2-6
Baseline CVN Properties

Material Identity	Material	T_{30} °F (°C)	T_{50} °F (°C)	T_{35mil} °F (°C)	Upper Shelf Energy (USE) ft-lb (J)
C2433-1 (LT orientation)	Susquehanna 1 Surveillance Plate	8.1 (-13.3)	35.4 (1.9)	19.7 (-6.8)	130.3 (176.7)
402K9171, 411L3071	Susquehanna 1 Surveillance Weld	-39.6 (-39.8)	2.2 (-16.6)	-9.4 (-23.0)	107.7 (146.0)

2.2.5 Tanh Curve Fits of CVN Test Data for Plate Heat C2433-1

PLATE HEAT C2433-1 (SH1)

CVGRAPH 5.0.2 Hyperbolic Tangent Curve Printed on 09/09/2002 08:33 AM
Page 1
Coefficients of Curve 1
A = 66.4 B = 63.9 C = 70.88 T0 = 53.93 D = 0.00E+00
Equation is A + B * [Tanh((T-To)/(C+DT))]
Upper Shelf Energy=130.3(Fixed) Lower Shelf Energy=2.5(Fixed)
Temp@30 ft-lbs=8.1 Deg F *Temp@50 ft-lbs=35.4 Deg F*
Plant: Susquehanna 1 Material: SA533B1 Heat: C2433-1
Orientation: LT Capsule: UNIRRA Fluence: 0.0 n/cm^2

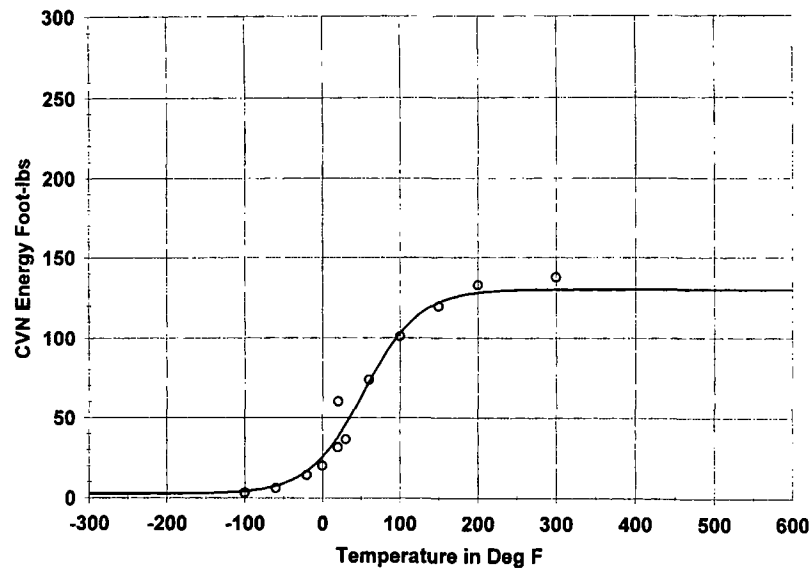

Charpy V-Notch Data

Temperature	Input CVN	Computed CVN	Differential
-100.00	3.00	4.14	-1.14
-60.00	6.00	7.44	-1.44
-20.00	14.00	16.62	-2.62
.00	20.00	25.40	-5.40
20.00	31.50	37.95	-6.45
20.00	60.00	37.95	22.05
30.00	36.50	45.61	-9.11
60.00	73.50	71.86	1.64
100.00	101.00	102.93	-1.93
150.00	120.00	122.33	-2.33
200.00	133.00	128.26	4.74

Figure 2-4
Charpy Energy Data for Plate C2433-1 (LT) Unirradiated

PLATE HEAT C2433-1 (SH1)

Page 2
Plant: Susquehanna 1 Material: SA533B1 Heat: C2433-1
Orientation: LT Capsule: UNIRRA Fluence: 0.0 n/cm^2

Charpy V-Notch Data

Temperature	Input CVN	Computed CVN	Differential
300.00	138.00	130.18	7.82

Correlation Coefficient = .987

Figure 2-4 (continued)
Charpy Energy Data for Plate C2433-1 (LT) Unirradiated (Continued)

2.2.6 Tanh Curve Fits of CVN Test Data for Weld Heat 402K9171, 411L3071

WELD HEAT 402K9171/411L3071 (SH1)

CVGRAPH 5.0.2 Hyperbolic Tangent Curve Printed on 09/09/2002 08:28 AM
Page 1
Coefficients of Curve 1
A = 55.1 B = 52.6 C = 99.07 T0 = 11.79 D = 0.00E+00
Equation is A + B * [Tanh((T-To)/(C+DT))]
Upper Shelf Energy=107.7(Fixed) Lower Shelf Energy=2.5(Fixed)
Temp@30 ft-lbs=-39.6 Deg F Temp@50 ft-lbs=2.2 Deg F
Plant: Susquehanna 1 Material: SMAW Heat: 402K9171/411
Orientation: NA Capsule: UNIRRA Fluence: 0.0 n/cm^2

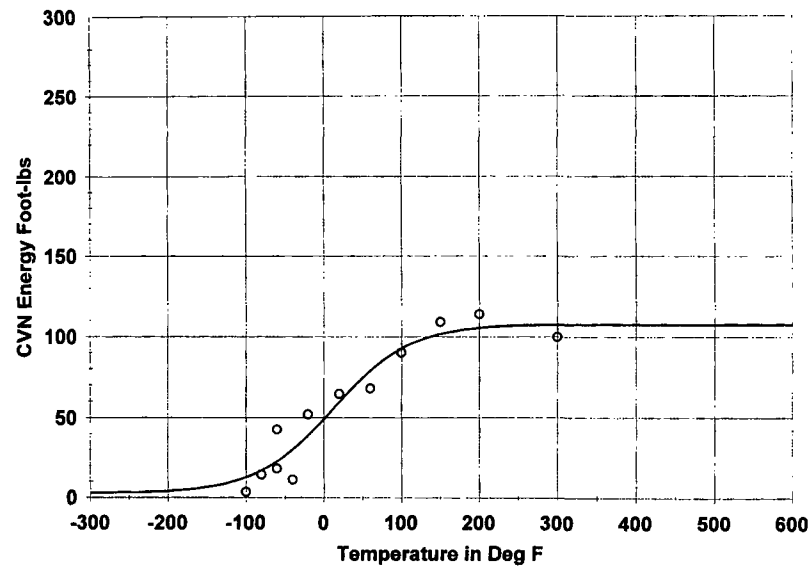

Charpy V-Notch Data

Temperature	Input CVN	Computed CVN	Differential
-100.00	3.50	12.47	-8.97
-80.00	14.00	16.76	-2.76
-60.00	42.50	22.50	20.00
-60.00	18.00	22.50	-4.50
-40.00	11.00	29.86	-18.86
-20.00	52.00	38.78	13.22
20.00	64.50	59.45	5.05
60.00	68.00	78.85	-10.85
100.00	90.00	92.53	-2.53
150.00	109.00	101.61	7.39
200.00	114.00	105.40	8.60

Figure 2-5
Charpy Energy Data for Weld 402K9171, 411L3071 Unirradiated

WELD HEAT 402K9171/411L3071 (SH1)

Page 2
Plant: Susquehanna 1 Material: SMAW Heat: 402K9171/411
Orientation: NA Capsule: UNIRRA Fluence: 0.0 n/cm^2

Charpy V-Notch Data

Temperature	Input CVN	Computed CVN	Differential
300.00	100.00	107.39	-7.39

Correlation Coefficient = .961

Figure 2-5 (continued)
Charpy Energy Data for Weld 402K9171, 411L3071 Unirradiated (Continued)

2.3 Capsule Opening

The 120° surveillance capsule was opened on October 8, 2012. As shown in Figures 2-2 and 2-3, the 120° capsule consisted of a single basket attached to the lead tube. The outside of the capsule had identification markings which could be clearly read. The capsule basket was engraved with the following markings:

Side Facing Vessel	*Side Facing Core*
Reactor 47	BDE6-004
131C7717G2	TDLP8-001
TBCE6-003	
TDLT2	

These markings are consistent with the markings observed on the 30° capsule basket described in [8]. As indicated in Figure 2-3, the capsule basket contained two Charpy packets and four tensile tubes.

Referring to Figure 2-2, the lead tube is positioned on the underside surface of the basket in the photograph. Therefore, the surface that is facing up in the photograph was oriented toward the vessel during irradiation. The hook at the top of the photograph is the vessel lower attachment hook, and it was below the capsule when the capsule was installed in the plant. The Charpy packet end tabs are on the left side in Figure 2-2. Moving up from the bottom of the capsule, the first item in the capsule was tensile tube G1 followed by tensile tubes G2, G3, and G4. Charpy packets G4 and G5 were position above the elevation of the G4 tensile tube, with Charpy packet G5 positioned at the highest elevation in the capsule.

Attention was paid to the location of the Charpy specimens and the dosimetry wire locations during disassembly of the Charpy packets. Each packet was found to contain one Fe, one Cu, and one Ni dosimetry wire located along the ends of the Charpy specimens at the locations shown in Figure 2-3. The wire locations along the ends of the Charpy specimens were on the bottom side of the Charpy packets when the capsule was in the plant. Therefore, the wires were irradiated in a horizontal position in the reactor. The identifications assigned to the dosimetry wires indicate the Charpy packet from which they were recovered. The wires and Charpy specimens were placed in individually marked containers for positive identification throughout the work.

Section 3: Neutron Fluence Calculation

The 120° capsule was irradiated in Susquehanna 1 for 17 cycles of operation. It was placed in the reactor's 120° capsule holder prior to cycle 1 and was removed following cycle 17 for a total irradiation period of 23.8 effective full power years (EFPY). The surveillance capsule included copper, iron, and nickel flux wire dosimetry specimens.

Evaluation of the surveillance capsule specimens requires knowledge of the neutron irradiation environment. The neutron flux density, neutron energy spectrum, and neutron fluence are required at the surveillance capsule location. The NRC has established guidelines in Regulatory Guide 1.190 [10] for determining best estimate values of flux, energy spectrum, and fluence for RPV damage assessments using particle transport methods. These guidelines are not specifically intended for use in surveillance capsule evaluations; however, the guidelines provide suitable guidance to support the development of accurate neutron transport analysis models for surveillance capsule evaluations.

This report documents the application of the modeling and analysis guidelines provided in [10] to determine the surveillance capsule accumulated irradiation and capsule specimen neutron fluence of the Susquehanna 1 120° ISP capsule flux wires. Additionally, the accumulated irradiation for the 30° capsule, removed at the end of cycle (EOC) 6, and 30° flux wires, removed at the end of cycle 1, were determined. The fast neutron fluence (E >1.0 MeV) was also calculated for the 30° capsule at the time of removal and for the 120° capsule at the end of cycle 17 and at the end of the reactor's extended design life of 54 EFPY. The fluence and activation values presented in this report were calculated using the RAMA Fluence Methodology [11] (hereinafter referred to as "RAMA"). The specific activities predicted by RAMA are compared to the activity measurements reported in Appendix A.

RAMA has been developed for the Electric Power Research Institute, Inc. (EPRI) and the BWRVIP for the purpose of calculating neutron fluence in Boiling Water Reactor (BWR) components. As prescribed in Regulatory Guide 1.190, RAMA has been benchmarked against industry standard benchmarks for both pressurized water reactor (PWR) and BWR designs. In addition, RAMA has been compared with several plant-specific dosimetry measurements and reported fluence from several commercial operating reactors. The results of the benchmarks and comparisons to measurements show that RAMA accurately predicts specimen activities, RPV fluence, and vessel internal component fluence in all light water reactor types. Under funding from EPRI and the BWRVIP, the

RAMA methodology has been reviewed by the U. S. NRC and subsequently given generic approval for determining fast neutron fluence in BWR pressure vessels [12] and vessel internal components that include the core shroud and top guide [13].

3.1 Description of the Reactor System

This section provides an overview of the reactor design and operating data inputs that were used to develop the Susquehanna 1 reactor fluence model. All reactor design and operating data inputs used to develop the model were plant-specific and were provided by PPL Susquehanna, LLC. The inputs for the fluence geometry model were developed from design and as-built drawings for the reactor pressure vessel, vessel internals, fuel assemblies, and containment regions. The reactor operating data inputs were developed from core simulator data that provided a historical accounting of how the reactor operated for cycles 1 through 17. Projections for cycle 18 to the end of the reactor's extended operating life were based on the reactor's operating history for cycle 17.

3.1.1 Reactor System Mechanical Design

Susquehanna 1 is a General Electric BWR/4 class reactor with a core loading of 764 fuel assemblies. Susquehanna 1 began commercial operation in 1983 with a design rated power of 3293 MWt. Power uprates were achieved in operating cycles 9, 13, 16 and 17 raising the thermal power output to 3441, 3489, 3733 and 3952 MWt, respectively. At the time of this fluence analysis, Susquehanna 1 had completed 17 cycles of operation.

Figure 3-1 illustrates the basic planar configuration of the Susquehanna 1 reactor at an axial elevation near the reactor core mid-plane. All of the radial regions of the reactor that are required for fluence projections are shown. Beginning at the center of the reactor and projecting outward, the regions include: the core region, including control rod locations and fuel assembly locations (fuel locations are shown only for the 0° to 90° quadrant); core reflector region (bypass water); central shroud wall; downcomer water region including the jet pumps; reactor pressure vessel (RPV) wall; cavity between RPV and insulation; insulation; cavity region between the insulation and biological shield; and biological shield (concrete wall).

The mechanical design inputs that were used to construct the Susquehanna 1 fluence geometry model included as-built and nominal design dimensional data. As-built data for the reactor components and regions of the reactor system is always preferred when constructing plant-specific models; however, as-built data is not always available. In these situations, nominal design information is used.

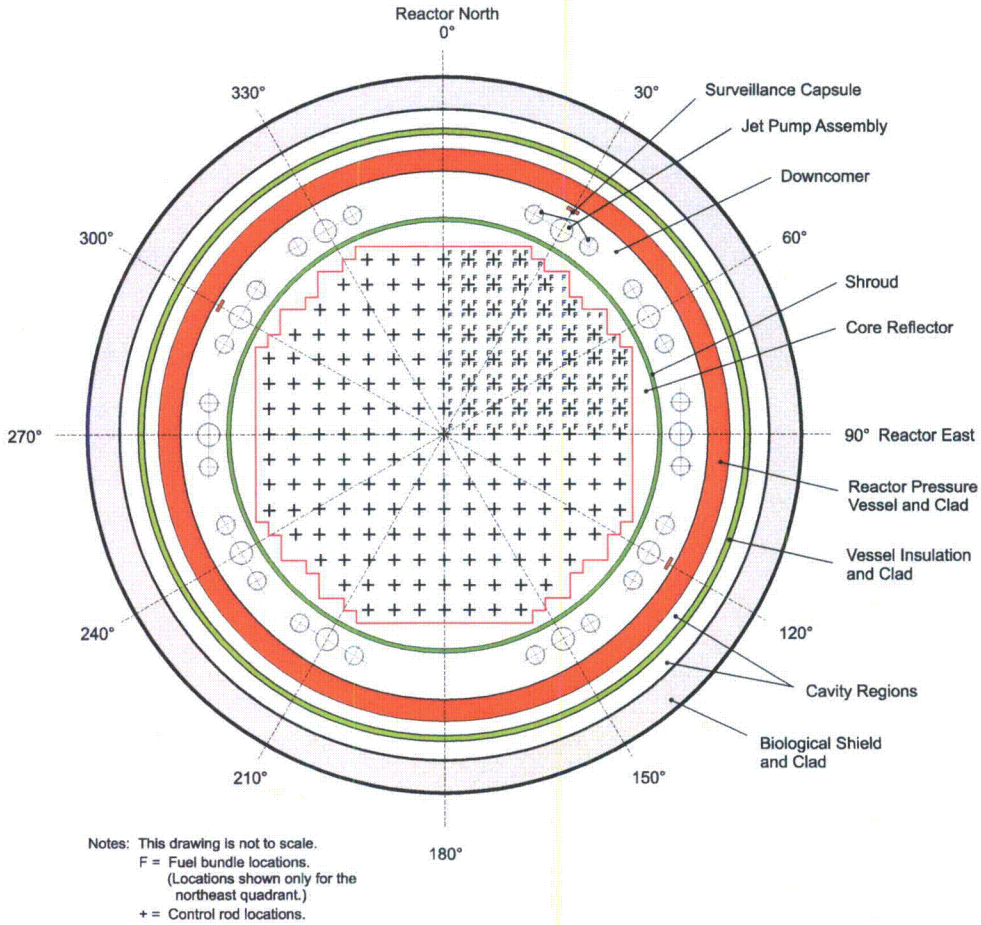

Figure 3-1
Planar View of Susquehanna 1 at the Core Mid-plane Elevation

For the Susquehanna 1 fluence model, the predominant dimensional information used to construct the fluence model was nominal design data. As-built data was used for the following dimensions:

- Upper, central, and lower shroud outer radii

Another important component of the fluence analysis is the accurate description of the surveillance capsules in the reactor. It is shown in Figure 3-1 that three surveillance capsules were initially installed in the Susquehanna 1 reactor. The capsules were attached radially to the inside surface of the RPV (looking outward from the core region) at the 30°, 120°, and 300° azimuths. Surveillance capsules are used to monitor the radiation accumulated in the reactor over a period of time. The importance of surveillance capsules in fluence analyses is that they contain flux wires that are irradiated during reactor operation. When a capsule is removed from the reactor, the irradiated flux wires are evaluated to obtain activity measurements. These measurements are used to validate the fluence model. Three sets of flux wires have been removed from the Susquehanna 1 reactor and analyzed. (See Section 3.3, which presents a comparison of the calculated-to-measured capsule results.)

3.1.2 Reactor System Material Compositions

Each region of the reactor is comprised of materials that include reactor fuel, steel, water, insulation, concrete, and air. Accurate material information is essential for the fluence evaluation as the material compositions determine the scattering and absorption of neutrons throughout the reactor system and, thus, affect the determination of neutron fluence in the reactor components.

Table 3-1 provides a summary of the materials for the various components and regions of the Susquehanna 1 reactor. The material attributes for the steel, insulation, concrete, and air compositions (i.e. material densities and isotopic concentrations) are assumed to remain constant for the operating life of the reactor. The attributes of the fuel compositions in the reactor core region change continuously during an operating cycle due to changes in power level, fuel burnup, control rod movements, and changing moderator density levels (voids). Because of the dynamics of the fuel attributes with reactor operation, several state-point data sets are used to describe the operating states of the reactor for each operating cycle. The number of data sets used in this analysis is presented in Section 3.1.3.3.

Table 3-1
Summary of Material Compositions by Region for Susquehanna 1

Region	Material Composition
Control Rods and Guide Tubes	Stainless Steel, B_4C
Core Support Plate	Stainless Steel
Fuel Support Piece	Stainless Steel
Fuel Assembly Lower Tie Plate	Stainless Steel, Zircaloy, Inconel
Reactor Core	^{235}U, ^{238}U, ^{239}Pu, ^{240}Pu, ^{241}Pu, ^{242}Pu, O_{fuel}, Zircaloy
Reactor Coolant/Moderator	Water
Core Reflector	Water
Fuel Assembly Upper Tie Plate	Stainless Steel, Zircaloy, Inconel
Top Guide	Stainless Steel
Core Spray Sparger Pipes	Stainless Steel
Core Spray Sparger Flow Areas	Steam
Shroud	Stainless Steel
Downcomer Region	Water
Jet Pump Riser and Mixer Flow Areas	Water
Jet Pump Riser and Mixer Metal	Stainless Steel
Jet Pump Riser Brace and Pads	Stainless Steel
Surveillance Capsule Specimens	Carbon Steel
Reactor Pressure Vessel Clad	Stainless Steel
Reactor Pressure Vessel Wall	Carbon Steel
Cavity Regions	Air (Nitrogen)
Insulation Clad	Stainless Steel
Insulation	Glass Wool
Biological Shield Clad	Carbon Steel
Biological Shield Wall	Reinforced Concrete

3.1.3 Reactor Operating Data Inputs

An accurate evaluation of reactor vessel and component fluence requires an accurate accounting of the reactor's operating history. The primary reactor operating parameters that affect the determination of fast neutron fluence in light water reactors include reactor power levels, core power distributions, coolant water density distributions, and fuel material (isotopic) distributions.

3.1.3.1 Core Loading

It is common in BWRs that more than one fuel assembly design may be loaded in the reactor core in any given operating cycle. For fluence evaluations, it is

important to account for the fuel assembly designs that are loaded in the core in order to accurately represent the neutron source distribution at the core boundaries (i.e. peripheral fuel locations and the top and bottom fuel elevations).

Four different fuel assembly mechanical designs were loaded in the Susquehanna 1 reactor during the period included in this evaluation. Table 3-2 provides a summary of the fuel mechanical designs loaded in the reactor core for each evaluated operating cycle. The cycle core loading provided by PPL Susquehanna, LLC was used to identify the fuel assembly designs in each cycle and their location in the core loading inventory. (Note that fuel loadings for cycles 14 and 15 were divided into two individual periods, identified as 14A, 14B, 15A and 15B.) For each cycle, appropriate fuel assembly models were used to build the reactor core region of the Susquehanna 1 RAMA fluence model.

3.1.3.2 Power History Data

Reactor power history is the measure of reactor power levels and core exposure on a continual or periodic basis. For this fluence evaluation, the power history for the Susquehanna 1 reactor was developed from power history inputs provided by PPL Susquehanna. The power history data showed that Susquehanna 1 started commercial operation with a design rated thermal power of 3293 MWt for cycles 1 through 8. Power uprates were implemented in cycles 9, 13, 16 and 17 raising the thermal power output to 3441, 3489, 3733 and 3952 MWt, respectively. It was assumed in this analysis that all future cycles would operate at the 3952 MWt power level.

The power history data for Susquehanna 1 included daily power levels for all cycles. This
data was used to calculate the capsule and vessel fluence. Periods of reactor shutdown due to refueling outages and other events were also accounted for in the model. The power history data was verified by comparing the calculated energy production in effective full power years with power production records provided by PPL Susquehanna, LLC. Table 3-3 lists the accumulated EFPY at the end of each cycle for this fluence evaluation.

Table 3-2
Summary of Susquehanna 1 Core Loading Inventory

Cycle	8x8 Designs		9x9 Designs	10x10 Designs	Dominant Peripheral Design
	GE5/GE6/ GE7	SPC	SPC	ATRIUM-10	
1	764				GE 8x8
2	572	192			GE 8x8
3	276	488			GE 8x8
4	36	488	240		SPC 8x8
5		296	468		SPC 8x8
6		76	688		SPC 8x8
7			764		SPC 9x9
8			764		SPC 9x9
9			764		SPC 9x9
10			764		SPC 9x9
11			456	308	SPC 9x9
12			200	564	SPC 9x9
13				764	ATRIUM-10
14A				764	ATRIUM-10
14B				764	ATRIUM-10
15A				764	ATRIUM-10
15B				764	ATRIUM-10
16				764	ATRIUM-10
17				764	ATRIUM-10
18+[1]				764	ATRIUM-10

3.1.3.3 Reactor State-Point Data

Core simulator data was provided by PPL Susquehanna, LLC to characterize the historical operating conditions of Susquehanna 1 for cycles 1 through 17 and cycle projections. The data calculated with core simulator codes represents the best-available information about the reactor core's operating history over the reactor's operating life. In this analysis, the core simulator data was processed by TransWare to generate state-point data files for input to the RAMA fluence model. The state-point files included three-dimensional data arrays that

[1] Cycles 18 and beyond use cycle 17 data for projecting fluence to the end of the extended plant license period.

described core power distributions, fuel exposure distributions, fuel materials (isotopics), and coolant water densities.

A separate neutron transport calculation was performed for each of the state points tallied in Table 3-3. The calculated neutron flux for each state point was combined with the appropriate power history data described in Section 3.1.3.2 in order to provide an accurate accounting of the fast neutron fluence for the reactor pressure vessel. Fluence projections to the end of the reactor's design life and extended design life were performed using projected equilibrium cycles. Equilibrium cycles are discussed below in "Projected Reactor Operation".

3.1.3.4 Beginning of Operation through Cycle 17 State Points

A total of 269 state points were used to represent the operating history for the first 17 operating cycles of Susquehanna 1. These state points were selected from hundreds of exposure points that were calculated with the core simulator code. The hundreds of exposure points were evaluated and grouped into a fewer number of exposure ranges in order to reduce the number of transport calculations required to perform the fluence evaluation. Several criteria were used in the determination of the exposure ranges, including evaluations of core thermal powers, core flows, core power profiles, and control rod patterns. In determining exposure ranges, it is assumed that there will be at least one exposure step in that range that would accurately represent the average operating conditions of the reactor over that range. This single exposure step is then referred to as the "state point". Table 3-3 shows the number of state points used for each cycle in this fluence evaluation.

3.1.3.5 Projected Reactor Operation

Projections of plant operations beyond cycle 17 are represented with an "equilibrium" cycle that incorporates the best-available information on expected cycle length, fuel bundle loading, and operating strategies for future cycles. Cycle 17, at a thermal power level of 3952 MWt, is used as the equilibrium cycle for this analysis to project fluence to the end of the extended plant design life of 54 EFPY.

Table 3-3
State-point Data for Each Cycle of Susquehanna 1

Cycle Number	Number of State Points	Rated Thermal Power[2] (MWt)	Accumulated Effective Full Power Years (EFPY)
1	15	3293	1.3
2	9	3293	2.0
3	15	3293	3.1
4	14	3293	4.3
5	12	3293	5.4
6	13	3293	6.6
7	13	3293	7.8
8	10	3293	8.9
9	12	3441	10.1
10	16	3441	11.5
11	20	3441	13.1
12	16	3441	14.9
13	18	3489	16.7
14A	19	3489	18.2
14B	9	3489	18.5
15A	11	3489	19.9
15B	7	3489	20.3
16	20	3733	22.1
17	20	3952	23.8
18+[3]	20	3952	54.0

[2] The rated thermal power is listed for each cycle. The actual power levels were used for the individual state-point calculations for cycles 1-17.

[3] Cycles 18 and beyond use cycle 17 data for projecting fluence to the end of the extended plant license.

3.1.3.6 Limitation of Fluence Projections

Some of the fluence values presented in this report are based on projections of Susquehanna 1 operations beyond the current operating cycle. Projections are performed using an assumed equilibrium cycle. The significance of the equilibrium cycle is that it defines the flux profiles that are used to project fluence into the future. Providing that the design basis for the equilibrium cycle does not change appreciably, projections based on the equilibrium cycle should remain bounding through 54 EFPY to support licensing, in-service inspection, and flaw evaluation activities.

If the design basis for the equilibrium cycle changes at any point in time, thereby producing a significant change to the flux profiles for the equilibrium cycle, then a new evaluation is needed. Operating conditions, if changed, that could impact the validity of the equilibrium cycle include power uprates, introduction of new fuel designs, changes in projected cycle lengths, changes in core loading strategies, changes in reactor flow, or other changes that could alter the flux profiles used in the fluence projections.

3.2 Calculation Methodology

The Susquehanna 1 evaluation was performed using the RAMA Fluence Methodology software package [11]. RAMA and its application to the Susquehanna 1 reactor are described in this section.

3.2.1 Description of the RAMA Fluence Methodology

The RAMA Fluence Methodology (RAMA) is a system of computer codes, a data library, and an uncertainty methodology that determines best-estimate fluence in light water reactor pressure vessels and vessel components. The primary codes that comprise the RAMA methodology include model builder codes, a particle transport code, and a fluence calculator code. The data library contains nuclear cross sections and response functions that are needed for each of the codes. The uncertainty methodology is used to determine the uncertainty and bias in the best-estimate fluence calculated by the software.

The primary inputs for RAMA are mechanical design parameters and reactor operating history data. The mechanical design inputs are obtained from plant-specific design drawings, which include as-built measurements when available. The reactor operating history data is obtained from reactor core simulator codes, system heat balance calculations, daily operating logs, and cycle summary reports that describe the operating conditions of the reactor over its operating lifetime. The primary outputs from RAMA calculations are neutron flux, neutron fluence, dosimetry activation, and an uncertainty evaluation.

The model builder codes consist of geometry and material processor codes that generate input for the particle transport code. The geometry model builder code uses mechanical design inputs and meshing specifications to generate three-dimensional geometry models of the reactor. The material processor code uses

reactor operating data inputs to process fuel materials, structural materials, and water densities that are consistent with the geometry meshing generated by the geometry model builder code.

The particle transport code performs three-dimensional neutron flux calculations using a deterministic, multigroup, particle transport theory method with anisotropic scattering. The primary inputs prepared by the user for the transport code include the geometry and material data generated by the model builder codes and numerical integration and convergence parameters for the iterative transport calculation. The transport solver is coupled with a general geometry modeling capability based on combinatorial geometry techniques. The coupling of general geometry with a deterministic transport solver provides a flexible, accurate, and efficient tool for calculating neutron flux in light water reactor pressure vessels and vessel components. The primary output from the transport code is the neutron flux in multigroup form.

The fluence calculator code determines fluence and activation in the reactor pressure vessel and vessel components over specified periods of reactor operation. The primary inputs to the fluence calculator include the multigroup neutron flux from the transport code, response functions for the various materials in the reactor, reactor power levels for the operating periods of interest, the specification of which components to evaluate, and the energy ranges of interest for evaluating neutron fluence. The fluence calculator includes treatments for isotopic production and decay that are required to calculate specific activities for irradiated materials. The reactor operating history is generally represented with several reactor state points that represent the various power levels and core power shapes generated by the reactor over the life of the plant. These detailed state points are combined with the daily reactor power levels to produce accurate estimates of the fluence and activations accumulated in the plant.

The uncertainty methodology provides an assessment of the overall accuracy of the RAMA Fluence Methodology. Variances in the dimensional data, reactor operating data, dosimetry measurement data, and nuclear data are evaluated to determine if there is a statistically significant bias in the calculated results that might affect the determination of the best-estimate fluence for the reactor. The plant-specific results are also weighted with comparative results from experimental benchmarks and other plant analyses and analytical uncertainties pertaining to the methodology to determine if the plant-specific model under evaluation is statistically acceptable as defined in Regulatory Guide 1.190.

The RAMA nuclear data library contains atomic mass data, nuclear cross-section data, and response functions that are needed in the material processing, transport, fluence, and reaction rate calculations. The cross-section data and response functions are based on the BUGLE-96 nuclear data library [14] and the VITAMIN-B6 data library [15].

The RAMA Fluence Methodology is described in the Theory Manual [16]. The general procedures for using the methodology are presented in the Procedures Manual [17].

3.2.2 RAMA Geometry Model for the Susquehanna 1 Reactor

Section 3.1 describes the design inputs that were provided by PPL Susquehanna, LLC for the Susquehanna 1 reactor fluence evaluation. These design inputs were used to develop a plant-specific, three-dimensional computer model of the Susquehanna 1 reactor with the RAMA Fluence Methodology.

Figures 3-2 and 3-3 provide general illustrations of the primary components, structures and regions developed for the Susquehanna 1 fluence model. Figure 3-2 shows the planar configuration of the reactor model at an elevation corresponding to the reactor core mid-plane elevation. Figure 3-3 shows an axial configuration of the reactor model. Note that the figures are not drawn to scale. They are intended only to provide a perspective for the layout of the model, and specifically how the various components, structures, and regions lie relative to the reactor core region (i.e., the neutron source).

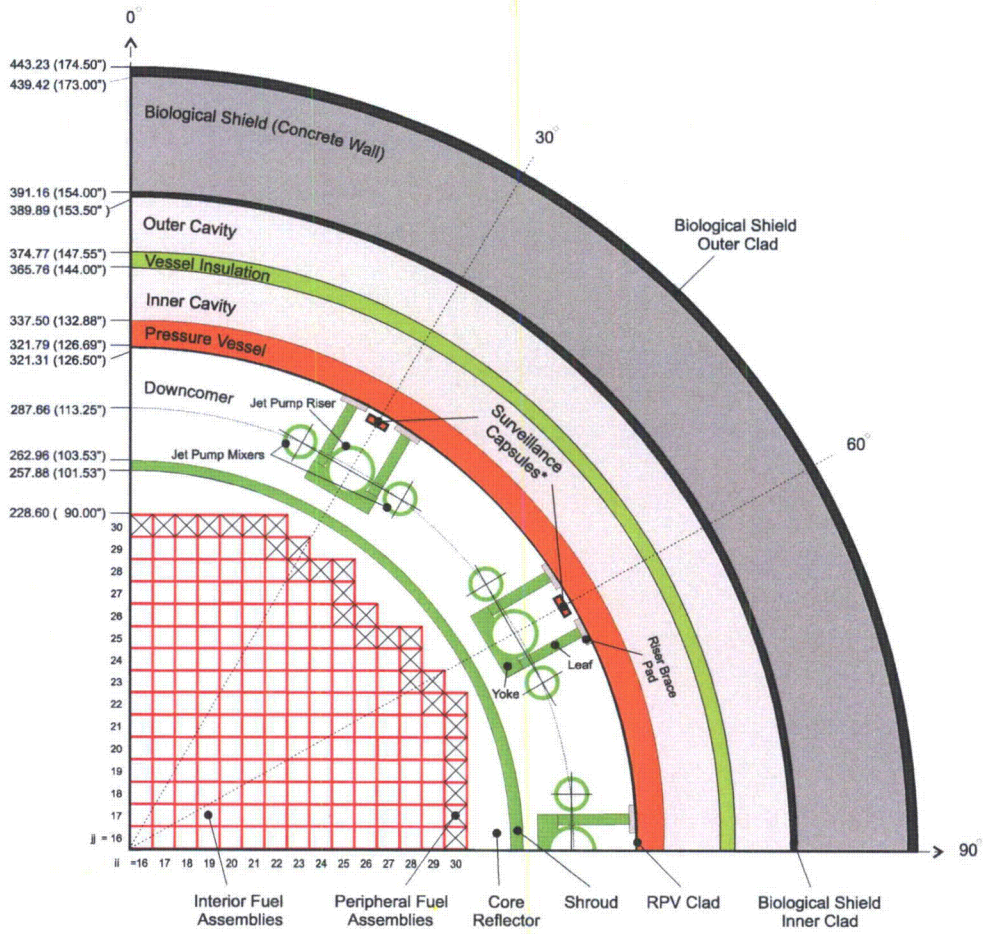

Figure 3-2
Planar View of the Susquehanna 1 RAMA Quadrant Model at the Core Mid-plane Elevation

Because the figures are intended only to provide a general overview of the model, they do not include illustrations of the geometry meshing developed for the model. To provide such detail is beyond the scope of this document.

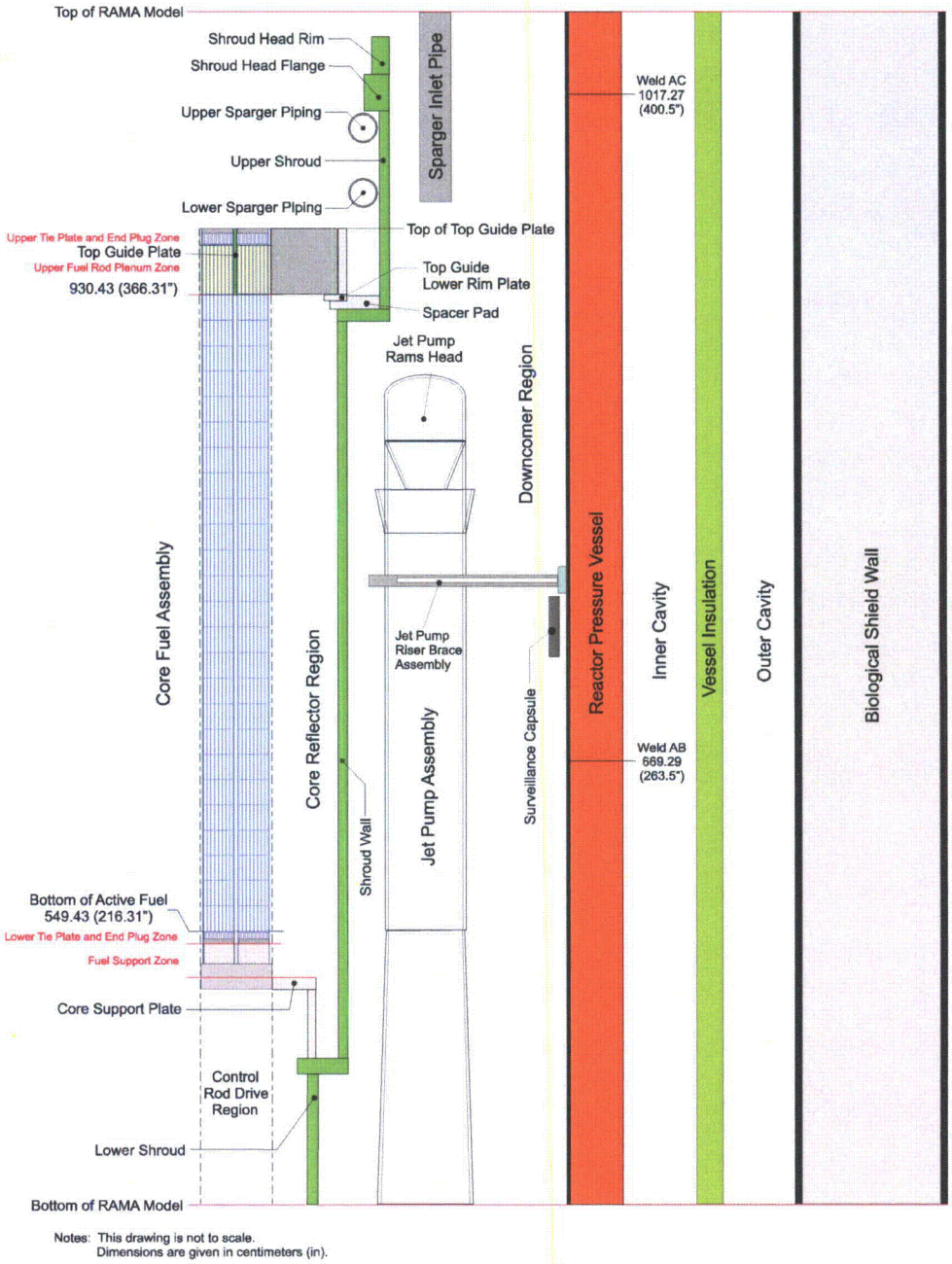

Figure 3-3
Axial View of the Susquehanna 1 RAMA Model

The following subsections provide an overview of the computer models that were developed for the various components, structures, and coolant flow regions of the Susquehanna 1 reactor.

3.2.2.1 Geometry Model

RAMA uses a generalized three-dimensional geometry modeling system that is based on a combinatorial geometry technique, which is mapped to a Cartesian coordinate system. In this analysis, an axial plane of the reactor model is defined by the (x,y) coordinates of the modeling system and the axial elevation at which a plane exists is defined along a perpendicular z-axis of the modeling system. Thus, any point in the reactor model can be addressed by specifying the (x,y,z) coordinates for that point.

Figure 3-1 illustrates a planar cross-section view of the Susquehanna 1 reactor design at an axial elevation corresponding to the reactor core mid-plane elevation. It is shown for this one elevation that the reactor design is a complex geometry composed of various combinations of rectangular, cylindrical, and wedge-shaped bodies. When the reactor is viewed in three dimensions, the varying heights of the different components, structures, and regions create additional geometry modeling complexities. An accurate representation of these geometrical complexities in a predictive computer model is essential for calculating accurate, best-estimate fluence in the reactor pressure vessel, the vessel internals, and the surrounding structures.

Figures 3-2 and 3-3 provide general illustrations of the planar and axial geometry complexities that are represented in the Susquehanna 1 fluence model. For comparison purposes, the planar view illustrated in Figure 3-2 corresponds to the same core mid-plane elevation illustrated in Figure 3-1. The computer model for Susquehanna 1 assumes azimuthal quadrant symmetry in the planar dimension.

Figure 3-2 illustrates the quadrant geometry that was modeled in this analysis. In terms of the modeling coordinate system, the "northeast" quadrant of the geometry is represented in the model. The 0° azimuth, which has a "north" designation, corresponds to the 0° azimuth referenced in the plan drawings for the reactor pressure vessel. Degrees are incremented clockwise. Thus, the 90° azimuth is designated as the "east" direction. All other components, structures, and regions have been appropriately mirror reflected or rotated to this quadrant based upon their relationship to the pressure vessel orientation to ensure that the fluence is appropriately calculated relative to the neutron source (i.e., the core region). Although symmetry is a modeling consideration, the results presented in this report for the different components and structures are given at their correct azimuths in the plant.

Figure 3-3 illustrates the axial configuration of the primary components, structures, and regions in the fluence model. For discussion purposes, the same components, structures, and regions shown in the planar view of Figure 3-2 are also illustrated in Figure 3-3. Figure 3-3 shows that the axial height of the fluence model spans from a lower elevation just below the jet pump riser inlet to above the core shroud head flange. This axial height covers all areas of the reactor pressure vessel that are expected to exceed a fluence threshold of 1.0E+17 n/cm^2 at 54 EFPY.

As previously noted, Figures 3-2 and 3-3 are not drawn precisely to scale. They are intended only to provide a perspective of how the various components, structures, and regions of the reactor are positioned relative to the reactor core region (i.e., the neutron source) and each other. The following subsections provide details on the modeling of individual components, structures, and regions. Please refer to the figures for visual orientation of the components and regions described in the following subsections.

3.2.2.2 Reactor Core and Core Reflector Models

The reactor core contains the nuclear fuel that is the source of the neutrons that irradiate all components and structures of the reactor. The core is surrounded by a shroud structure that serves to channel the reactor coolant through the core region during reactor operation. The region between the core and the core shroud is the core reflector, and it contains coolant. The reactor core geometry is rectangular in design and is modeled with rectangular elements to preserve its shape in the analysis. The core reflector region interfaces with the rectangular shape of the core region and the curved shape of the core shroud. It is, therefore, modeled using a combination of rectangular and cylindrical elements.

The core region is centered in the reactor pressure vessel and is characterized in the analysis with two fundamental fuel zones: interior fuel assemblies and peripheral fuel assemblies. The peripheral fuel assemblies are the primary contributors to the neutron source in the fluence calculation. Because these assemblies are loaded at the core edge where neutron leakage from the core is greatest, there is a sharp power gradient across these assemblies that requires consideration. To account for the power gradient, the peripheral fuel assemblies are sub-meshed with additional rectangular elements that preserve the pin-wise details of the fuel assembly geometry and power distribution. The interior fuel assemblies make a lesser contribution to the reactor fluence and are, therefore, modeled in various homogenized forms in accordance with their contributions to the reactor fluence. For computational efficiency, homogenization treatments are used in the interior core region primarily to reduce the number of mesh regions that must be solved in the transport calculation. The meshing configuration for each fuel assembly location in the core region is determined by parametric studies to ensure an accurate estimate of fluence throughout all regions of the reactor system.

Each fuel assembly design, whether loaded in the interior or peripheral locations in the core, is represented with four axial material zones: the lower tie plate/end plug zone, the fuel zone, the fuel upper plenum zone, and the upper tie plate/end plug zone. The structural materials in the top and bottom nozzles for each unique assembly design are represented in the model to address the shielding effects that these materials have on the components above and below the core region. The fuel zone contains the nuclear fuel and structural materials for the fuel assemblies. The materials for each fuel assembly are unique during reactor operation and are incorporated into the model using reactor operating data from core simulator codes. The upper plenum region captures fission gases during reactor operation.

The Susquehanna 1 reactor core region has a nominal elevation for the bottom of active fuel at 549.43 cm (216.31 in.) and an active fuel height of 381.00 cm (150 in.). All Susquehanna 1 loaded fuel designs have active fuel heights of 381.0 cm (150 in.).

From an isotopic standpoint, the core is modeled using quadrant symmetry. For the 30° and 120° capsule evaluations, as well as the peak RPV fluence calculations, the NE fuel quadrant was used.

3.2.2.3 Core Shroud Model

The core shroud is a canister-like structure that contains the reactor core and channels the reactor coolant and steam produced by the core into the steam separators. Axially the shroud extends from the lower shroud wall to the top of the shroud head rim in the model. The core shroud is cylindrical in design and is modeled with pipe elements.

3.2.2.4 Downcomer Region Model

The downcomer region lies between the core shroud and the reactor pressure vessel. It is basically cylindrical in design, but with some geometrical complexities created by the presence of jet pumps and surveillance capsules in the region. The majority of the downcomer region is modeled with pipe segments. The areas of the downcomer containing the jet pumps and specimen capsules are modeled with the appropriate geometry elements to represent their design features and to preserve their radial, azimuthal, and axial placement in the downcomer region. These structures are described further in the following subsections.

3.2.2.5 Jet Pump Model

There are ten jet pump assemblies in the downcomer region of Susquehanna 1, which provide the main recirculation flow for the core. The jet pumps are modeled at azimuths 30°, 60°, and 90° in the downcomer region. When symmetry is applied to the model, the 30° location represents the jet pump assemblies that are positioned azimuthally at 30°, 150°, 210°, and 330°; the 60° location represents those at 60°, 120°, 240°, and 300°; and the 90° location represents the jet pump assemblies at 90° and 270°. Note that there are no jet pumps present at the 0° and 180° azimuths of the reactor.

The jet pump model includes representations for the riser, mixer, and diffuser pipes; nozzles; rams head; riser inlet pipe; and riser brace yoke, leafs, and pads. The jet pump assembly design is modeled using cylindrical pipe elements for the jet pump riser and mixer pipes. The riser pipe is correctly situated between the mixer pipes. The riser brace assembly model includes two leaf structures that attach to the yoke and pad elements.

3.2.2.6 Surveillance Capsule Model

Section 3.1 describes the three surveillance capsules installed in the Susquehanna 1 reactor. The surveillance capsules are installed near the inner surface of the pressure vessel wall. The surveillance capsules are rectangular in design. Because of this shape, the capsules are not easily implemented in the otherwise cylindrical elements of the downcomer region model. With reference to Figure 3-1, it is observed that the capsules are of small dimensions in the planar geometry and they reside a long distance (view factor) from the core region. Based on these factors, the otherwise rectangular shape of the surveillance capsules can be reasonably approximated in the model with arc elements. The surveillance capsule model also includes a representation for the downcomer water that surrounds the capsule on all sides.

The surveillance capsules are correctly modeled behind the jet pump riser pipes at the 30° and 60° azimuths. When symmetry is applied to the model, the 30° location represents the capsule installed at 30°, while the 60° location represents the capsules at 120° and 300°.

The surveillance capsules are modeled at their correct axial position and height relative to the core region. The surveillance capsules cover about nine percent of the total core height.

3.2.2.7 Reactor Pressure Vessel Model

The reactor pressure vessel and vessel cladding lie outside the downcomer region and each is cylindrical in design. Both are modeled with pipe elements. The cladding-pressure vessel interface is a key location for RPV fluence calculations and is preserved in the model. This interface defines the inside surface (0T) for the pressure vessel base metal where the RPV fluence is calculated. Susquehanna 1 has cladding only on the inside surface of the pressure vessel wall.

3.2.2.8 Vessel Insulation Model

The vessel insulation lies in the cavity region outside the pressure vessel wall. The insulation is cylindrical in design and follows the contour of the pressure vessel wall. It is modeled with pipe elements.

3.2.2.9 Inner and Outer Cavity Models

The cavity region lies between the pressure vessel and biological structures. As previously described, the vessel insulation lies in the cavity region; thus creating two cavity regions. The inner cavity region lies between the vessel and the insulation. The outer cavity region lies between the vessel insulation and biological shield cladding. The boundaries of the cavity regions follow the contours of the pressure vessel, vessel insulation, and biological shield. The cavity regions are essentially cylindrical in design and are modeled with pipe segments.

3.2.2.10 Biological Shield Model

The biological shield (concrete) defines the outer most region of the fluence model. The biological shield is basically cylindrical in design and is modeled with pipe segments. There is cladding on the inside and outside surfaces of the biological shield.

3.2.2.11 Above-Core Component Models

Figure 3-3 includes illustrations of other components and regions that lie above the reactor core region. The predominant above-core components represented in the model include the top guide and core spray spargers.

3.2.2.11.1 Top Guide Model

The top guide component lies above the core region. The top guide is appropriately modeled by including representations for the vertical fuel assembly parts and top guide plates. The upper fuel assembly parts that extend into the top guide region are modeled in three axial segments: the fuel rod plenum, fuel rod upper end plugs, and fuel assembly upper tie plate. The fuel assembly parts and top guide plates are modeled with rectangular elements.

3.2.2.11.2 Core Spray Sparger Model

The core spray spargers include upper and lower sparger pipes and a vertical inlet pipe. The core spray spargers are appropriately represented as torus structures in the model. The sparger pipes reside inside the upper shroud wall above the top guide. The spargers are modeled as pipe-like structures and include a representation of reactor coolant inside the pipes.

3.2.2.12 Below-Core Component Models

Figure 3-3 includes illustrations of other components and regions that lie below the reactor core region. The fuel support piece, core support plate, and core inlet regions appropriately include a representation of the cruciform control rod below the core region. The lower fuel assembly parts include representations for the fuel rod lower end plugs, lower tie plate, and nose piece. The below-core components are modeled with rectangular elements with the exception of the core support plate. The core support plate is modeled using both rectangular and cylindrical elements to provide an appropriate representation of that component.

3.2.2.13 Summary of the Geometry Modeling Approach

To summarize the reactor modeling process, there are several key features of the RAMA code system that allow the reactor design to be accurately represented for RPV and capsule fluence evaluations. Following is a summary of some of the key features of the model.

- Rectangular, cylindrical, and wedge bodies are mixed in the model in order to provide an accurate geometrical representation of the components and regions in the reactor.
- The reactor core geometry is modeled with rectangular bodies to represent its actual shape in the reactor. The fuel assemblies in the core region are also sub-meshed with additional rectangular bodies to represent the pin cell regions in the assemblies.
- A combination of rectangular and cylindrical bodies is used to describe the transition parts between the rectangular core region and the cylindrical outer core regions.
- Cylindrical and wedge bodies are used to model the components and regions that extend outward from the core region (core shroud, downcomer, RPV, etc.).
- The surveillance capsules are modeled at their correct radial, azimuthal, and elevational positions behind the jet pumps in the downcomer region.
- The above-core region includes accurate representations of the top guide and core spray spargers.
- The below-core region includes appropriate representations for the fuel support piece, core support plate, core inlet regions, cruciform control rods, and control rod drives.
- The biological shield is appropriately represented as a cylindrical body.

3.2.3 RAMA Calculation Parameters

The RAMA transport code uses a three-dimensional deterministic transport method to calculate the neutron flux. The accuracy of the transport method is based on a numerical integration technique that uses ray-tracing to characterize the geometry, anisotropy treatments to determine the directional flow of particles, and convergence parameters to determine the overall accuracy of the flux solution between iterates. The code allows the user to specify values for each of these parameters.

The primary input parameters that control the ray-tracing calculation are the distance between parallel rays in the planar and axial dimensions, the depth that a particle is tracked when a reflective boundary is encountered, and the number of equally spaced angles in polar coordinates for tracking the particles. Plant-specific values are determined for each of the parameters. The RAMA transport calculation employs a treatment for anisotropy that is based on a Legendre expansion of the scattering cross sections. By default, the RAMA transport calculation uses the maximum order of expansion that is available for each nuclide in the RAMA nuclear data library. For the actinide and zirconium nuclides, a P_5 expansion of the scattering cross sections is used. For all other nuclides, a P_7 expansion of the scattering cross sections is used.

The overall accuracy of the neutron flux calculation is determined using an iterative technique to converge the flux iterations. The convergence criterion used

in the evaluation was determined by parametric study to provide an asymptotic solution for this model.

3.2.4 RAMA Neutron Source Calculation

RAMA calculates a unique neutron source distribution for each transport calculation using the input relative power density factors for the fuel region and data from the RAMA nuclear data library. The source distribution changes with fuel burnup; thus, the source is determined using core-specific three-dimensional burnup distributions at frequent intervals throughout a cycle. For the fluence model, the peripheral fuel assemblies are modeled to preserve the power gradient at the core edge that is formed from the pin-wise source distributions in these fuel assemblies.

3.2.5 RAMA Fission Spectra

RAMA calculates a weighted fission spectrum for each transport calculation that is based on the relative contributions of ^{235}U, ^{238}U, ^{239}Pu, ^{240}Pu, ^{241}Pu, and ^{242}Pu isotopes. The fission spectra for these isotopes are derived from the BUGLE-96 nuclear data library.

3.3 Surveillance Capsule Activation and Fluence Results

This section documents the fluence and activation results for the Susquehanna 1 reactor. The activation results also form the basis for the validation and qualification of the application of the RAMA Fluence Methodology to the Susquehanna 1 reactor in accordance with the requirements of Reg. Guide 1.190. Reg. Guide 1.190 requires fluence calculational methods to be validated by comparison with measurements from operating reactor dosimetry for the specific plant being analyzed or for reactors of similar design.

Three flux wire activation analyses were performed for the Susquehanna 1 reactor. Flux wires were removed from the 30° capsule flux wire holder and analyzed at the end of cycle 1 (irradiated for 1.3 EFPY); surveillance capsule flux wires were removed at the end of cycle 6 from the 30° capsule (irradiated for 6.6 EFPY); and surveillance capsule flux wires were removed at the end of cycle 17 from the 120° capsule (irradiated for 23.8 EFPY). Details of the dosimetry specimens and analysis are presented in Section 3.3.1.

Best estimate fast fluence (E >1.0 MeV) was calculated for each of the two removed capsules and the 30° capsule flux wire holder. Additionally, best estimate fast fluence was calculated for the 300° capsule still in the reactor in support of lead factor calculations. Lead factors are determined and reported for all capsules.

3.3.1 Comparison of Predicted Activation to Plant-specific Measurements

The comparison of predicted activation for the Susquehanna 1 cycles 1, 6, and 17 flux wires to measurements is presented in this subsection. Fluence values are also calculated and reported in Section 3.3.2 for each of the capsule flux wires.

3.3.1.1 Cycle 1 30° Flux Wire Holder Activation Analysis

Copper and iron flux wires were irradiated in the Susquehanna 1 surveillance capsule flux wire holder at the 30° azimuth during the first cycle of operation. The wires were removed after being irradiated for a total of 1.3 EFPY. Activation measurements were performed following irradiation for the following reactions [18]: ^{63}Cu (n, α) ^{60}Co and ^{54}Fe (n,p) ^{54}Mn. The precise location of the individual wires within the surveillance capsule flux wire holder is not known, therefore, the activation calculations were performed at the center of the holder.

Table 3-4 provides a comparison of the RAMA calculated specific activities and the measured specific activities for the flux wire specimens. The cycle 1 total flux wire average calculated-to-measured (C/M) value is 0.99 with a standard deviation of ±0.08.

Table 3-4
Comparison of Specific Activities for Susquehanna 1 Cycle 1 30° Flux Wire Holder Wires (C/M)

Flux Wires	Measured (Bq/mg)	Calculated (Bq/mg)	Calculated vs. Measured	Standard Deviation
Iron				
Fe-1	37.84	40.46	1.07	–
Fe-2	37.96	40.46	1.07	–
Fe-3	38.28	40.46	1.06	–
Average	38.03	40.46	1.06	0.01
Copper				
Cu-1	2.102	1.945	0.93	–
Cu-2	2.149	1.945	0.91	–
Cu-3	2.144	1.945	0.91	–
Average	2.132	1.945	0.91	0.01
Total Flux Wire Average	**---**	**---**	**0.99**	**0.08**

3.3.1.2 Cycle 6 30° Surveillance Capsule Activation Analysis

Copper, iron, and nickel flux wires were irradiated in the Susquehanna 1 surveillance capsule
at the 30° azimuth during the first 6 cycles of operation. The wires were removed after being irradiated for a total of 6.6 EFPY. Activation measurements were performed following irradiation for the following reactions [8]: ^{63}Cu (n, α) ^{60}Co, ^{54}Fe (n,p) ^{54}Mn, and ^{58}Ni (n,p) ^{58}Co. The precise location of the individual wires within the surveillance capsule flux wire holder is not known, therefore, the activation calculations were performed at the center of the holder.

Table 3-5 provides a comparison of the RAMA calculated specific activities and the measured specific activities for the surveillance capsule flux wire specimens. The cycle 6 capsule total flux wire average C/M value is 0.96 with a standard deviation of ±0.06.

Table 3-5
Comparison of Specific Activities for Susquehanna 1 Cycle 6 30° Surveillance Capsule Flux Wires (C/M)

Flux Wires	Measured (dps/g)	Calculated (dps/g)	Calculated vs. Measured	Standard Deviation
Iron				
G1	7.16E+04	7.48E+04	1.04	–
G2	7.79E+04	7.48E+04	0.96	–
G3	7.72E+04	7.48E+04	0.97	–
Average	7.56E+E4	7.48E+04	0.99	0.05
Copper				
G1	8.09E+03	7.67E+03	0.95	–
G2	8.79E+03	7.67E+03	0.87	–
G3	8.80E+03	7.67E+03	0.87	–
Average	8.56E+03	7.67E+03	0.90	0.04
Nickel				
G1	1.08E+06	1.14E+06	1.06	–
G2	1.18E+06	1.14E+06	0.97	–
G3	1.18E+06	1.14E+06	0.97	–
Average	1.15E+06	1.14E+06	1.00	0.05
Total Flux Wire Average	**---**	**---**	**0.96**	**0.06**

3.3.1.3 Cycle 17 120° Surveillance Capsule Activation Analysis

Copper, iron, and nickel flux wires were irradiated in the Susquehanna 1 surveillance capsule at the 120° azimuth during the first 17 cycles of operation. The wires were removed after being irradiated for a total of 23.8 EFPY. Activation measurements were performed following irradiation for the following reactions (see Appendix A): ^{63}Cu (n, α) ^{60}Co, ^{54}Fe (n,p) ^{54}Mn, and ^{58}Ni (n,p) ^{58}Co.

Table 3-6 provides a comparison of the RAMA calculated specific activities and the measured specific activities for the surveillance capsule flux wire specimens. The cycle 17 capsule total flux wire average C/M value is 0.99 with a standard deviation of ±0.06.

Table 3-6
Comparison of Specific Activities for Susquehanna 1 Cycle 17 120° Surveillance Capsule Flux Wires (C/M)

Flux Wires	Measured (dps/mg)	Calculated (dps/mg)	Calculated vs. Measured	Standard Deviation
Iron				
Fe-G4	70.09	74.80	1.07	–
Fe-G5	77.62	74.80	0.96	–
Average	73.86	74.80	1.02	0.07
Copper				
Cu-G4	12.17	11.83	0.97	–
Cu-G5	13.11	11.83	0.90	–
Average	12.64	11.83	0.94	0.05
Nickel				
Ni-G4	1137.91	1139.70	1.00	–
Ni-G5	1088.86	1139.70	1.05	–
Average	1113.39	1139.70	1.02	0.03
Total Flux Wire Average	**---**	**---**	**0.99**	**0.06**

3.3.1.4 Surveillance Capsule Activation Analysis Summary

Table 3-7 presents a summary of the total average calculated-to-measured result of specific activities for all Susquehanna 1 flux wires. Combining all flux wires (copper, iron, and nickel), the total average C/M is 0.98 with a standard deviation of ±0.07.

Table 3-7
Comparison of Activities for Susquehanna 1 Flux Wires

Dosimeter	Number of Measurements	Calculated vs. Measured	Standard Deviation
30° Flux Wire (EOC 1)	6	0.99	0.08
30° Capsule (EOC 6)	9	0.96	0.06
120° Capsule (EOC 17)	6	0.99	0.06
Total	**21**	**0.98**	**0.07**

3.3.2 Capsule Peak Fluence Calculations and Lead Factor Determinations

Best estimate fast neutron fluence was calculated for each of the capsules originally installed in the Susquehanna 1 reactor. Two of the three original capsules (the 30° and 120°) have been removed; the third capsule, located at 300°, remains in the reactor. The fluences for the 30° and 120° capsules are reported at the time of capsule removal, while the 300° capsule has fluence reported at the end of the reactor's extended operating life of 54 EFPY. Additionally, the lead factor for each capsule is calculated by dividing the peak capsule fluence by the respective peak RPV fluence at a given reporting time. The results of these calculations are presented in Table 3-8. Note that since the 300° capsule has not yet been removed, the lead factor and fluence are estimated.

It is observed in Table 3-8 that the lead factors vary between cycles and capsules. In theory, a plant running with a consistent fuel loading pattern and a symmetric power shape will have similar lead factors for all capsules, since the capsules usually reside in symmetric locations. Like other fluence predictions, any future changes in any of the items listed in Section 3.1.3.6 (Limitation of Fluence Projections) will impact the 300° capsule lead factor predictions.

Table 3-8
Calculated Capsule Fast Neutron Fluence and Lead Factors for Susquehanna 1

Capsule	Time of Removal	EFPY at Removal	Capsule Fluence (n/cm^2)	RPV Peak Fluence (n/cm^2)	Lead Factor
30°	EOC 6	6.6 EFPY	1.64E+17	1.54E+17	1.06
120°	EOC 17	23.8 EFPY	5.75E+17	5.46E+17	1.05
300°	EOXL[4] (est.)	54 EFPY	1.37E+18	1.28E+18	1.07

[4] EOXL represents the end of the extended design life, which is assumed to represent 54 EFPY.

3.4 Capsule Fluence Uncertainty Analysis

This section presents the combined uncertainty analysis and bias determination for the Susquehanna 1 capsule fluence evaluation. The combined uncertainty is comprised of the comparison uncertainty factors developed in Section 3.3, *Surveillance Capsule Activation and Fluence Results*, and an analytic uncertainty factor developed in this section. When combined, these components provide a basis for determining the overall uncertainty (1σ) and bias in the capsule fluence for this analysis.

The requirements for determining the combined uncertainty and bias for light water reactor fluence evaluations are provided in Regulatory Guide 1.190. The method implemented for determining the combined uncertainty and bias for reactor component fluence is described in the RAMA Theory Manual [16]. Regarding the determination of a bias in the fluence, Regulatory Guide 1.190 provides that an adjustment to the calculated fluence for bias effects is needed if a statistically significant bias exists in the fluence computation.

The results presented in this section show that the combined uncertainty for the Susquehanna 1 capsule fluence evaluation is 11.9% and that no adjustment for bias effects is required to the calculated capsule fluence reported in Section 3.3 of this report.

The following subsections describe the comparison uncertainties determined in Section 3.3, the determination of the analytic uncertainty, and the determination of the overall combined uncertainty and bias for the Susquehanna 1 capsule fluence evaluation.

3.4.1 Comparison Uncertainty

Comparison uncertainty factors are determined by comparing calculated activities with activity measurements. For capsule fluence evaluations, two comparison uncertainty factors are considered: an operating reactor comparison uncertainty factor and a benchmark comparison uncertainty factor. The determination of a comparison uncertainty factor based on measurements involves the combination of two measurement components. One component is the variation in the comparison of the calculated-to-measured (C/M) activity ratio and the other accounts for the uncertainty introduced by the measurement process.

3.4.1.1 Operating Reactor Comparison Uncertainty

The operating reactor, or plant-specific, comparison uncertainty for the Susquehanna 1 reactor is determined by combining the standard deviation for the activity comparisons with the measurement uncertainty for the plant-specific activity measurements.

3.4.1.2 Benchmark Comparison Uncertainty

The benchmark comparison uncertainty used in the Susquehanna 1 uncertainty analysis is based on a set of industry standard simulation benchmark comparisons.

3.4.2 Analytic Uncertainty

The calculational models used for fluence analyses are comprised of numerous analytical parameters that have associated uncertainties in their values. The uncertainty in these parameters needs to be tested for its contribution to the overall fluence uncertainty.

The uncertainty values for the geometry parameters are based upon uncertainties in the dimensional data used to construct the plant geometry model. The uncertainty values for the material parameters are based upon uncertainties in the material densities for the water and nuclear fuel materials and the compositional makeup of typical steel materials.

The uncertainty values for the fission source parameters are based upon uncertainties in the fuel exposure and power factors for the fuel assemblies loaded on the core periphery. The transport method used in the fluence analysis employs a fission source calculation that accounts for the relative contributions of the uranium and plutonium fissile isotopes in the fuel and the relative power density of the fuel in the reactor. Both fission source parameters are derived directly from information calculated by three-dimensional core simulator codes. The uncertainty values for the nuclear cross-section parameters are based upon uncertainties in the number densities for the predominant nuclides that make up the reactor materials.

The uncertainty parameters for the fluence model inputs are based upon geometry meshing and numerical integration parameters used in the neutron flux transport calculation. The process for determining the geometry meshing and numerical integration parameters involves an exhaustive sensitivity study that is described in the RAMA Procedures Manual [17].

3.4.3 Combined Uncertainty

The combined uncertainty for the capsule fluence evaluation is determined with a weighting function that combines the analytic, plant-specific comparison, and benchmark comparison uncertainty factors developed in Sections 3.4.1 and 3.4.2, above. Table 3-9 shows that the combined uncertainty (1σ) determined for the Susquehanna 1 capsule fluence is 11.9% for energy >1.0 MeV.

Table 3-9 also shows that, in accordance with Regulatory Guide 1.190, no bias term exists and it is not necessary to adjust the RAMA predicted capsule fluence in this analysis for bias effects. It is also demonstrated in Table 3-9 that the combined uncertainty is within the limits prescribed in U. S. NRC Regulatory Guide 1.190 (i.e. ≤ 20%).

Table 3-9
Susquehanna 1 Capsule Uncertainty for Energy >1.0 MeV

Uncertainty Term	Value
Combined Uncertainty (1σ)	11.9%
Bias	None[5]

[5] The bias terms are less than their constituent uncertainty values, concluding that no statistically significant bias exists.

Section 4: Charpy Test Data

4.1 Charpy Test Procedure

Charpy impact tests were conducted in accordance with American Society for Testing and Materials (ASTM) Standards E185-82 [3] and E23-02 [19]. The 1982 version of E185 has been reviewed and approved by NRC for surveillance capsule testing applications. This standard references ASTM E23 [19]. The tests were conducted using a Tinius Olsen Testing Machine Company, Inc. Model 84 impact test machine with a 300 ft-lb (406.75 J) energy capacity. The Model 84 is equipped with a dial gage as well as the MPM optical encoder system for accurate absorbed energy measurement. The machine is also equipped with an instrumented striker, so a total of three independent measurements of the absorbed energy were made for every test. In all cases, the optical encoder measured energy was reported as the impact energy. The optical encoder energy is much more accurate than the analog dial. The optical encoder can resolve the energy to within 0.04 ft-lbs (0.054 J), whereas, for the dial, the resolution is around 0.25 ft-lbs (0.34 J). The impact energy was corrected for windage and friction for each test performed. The velocity of the striker at impact was nominally 18 ft/s (5.49 m/s). The MPM encoder system measures the exact impact velocity for every test. Calibration of the machine was verified as specified in ASTM E23, and verification specimens were obtained from the National Institute
for Standards and Technology (NIST) and tested in accordance with the standard.

The ASTM E23 procedure for specimen temperature control using an in-situ heating and cooling system was followed. Using the MPM in-situ heating/cooling technology, each specimen was thermally conditioned right up to the instant of impact; thermal losses associated with liquid bath systems, such as those resulting from transfer from a liquid bath to the test machine, were eliminated. Each specimen was held at the desired test temperature for at least 5 minutes prior to testing, and the fracture process zone temperature was held to within ± 1.8 F (± 1 C) up to the instant of strike. Precision calibrated tongs were used for specimen centering on the test machine.

Lateral expansion (LE) was determined from measurements made with a lateral expansion gage. The lateral expansion gage was calibrated using precision gage blocks which are traceable to NIST. The percentage of shear fracture area was determined by integrating the ductile and brittle fracture areas using the MPM Digital Optical Comparator (DOC) image analysis system. As shown in Figure

4-1, each fracture surface image is captured, outlined to delineate the brittle area, and outlined to define the outer ductile fracture region. The DOC software then performs a pixel area integration and automatically calculates the shear fracture area. This method for shear area determination is the most accurate method given in ASTM E23 and is superior to the commonly used photograph comparison method.

The number of Charpy specimens for measurement of the transition region and upper shelf was limited. Therefore, the choice of test temperatures was very important. Prior to testing, the Charpy energy-temperature curve was predicted using embrittlement models and previous data. The first test was then conducted near the middle of the transition region, and test temperature decisions were then made based on the test results. Overall, the goal was to perform two tests on the upper shelf, and to use the remaining specimens to characterize the 30 ft-lb (41 J) index. This approach was successful, and the transition region and upper shelf energy are well defined.

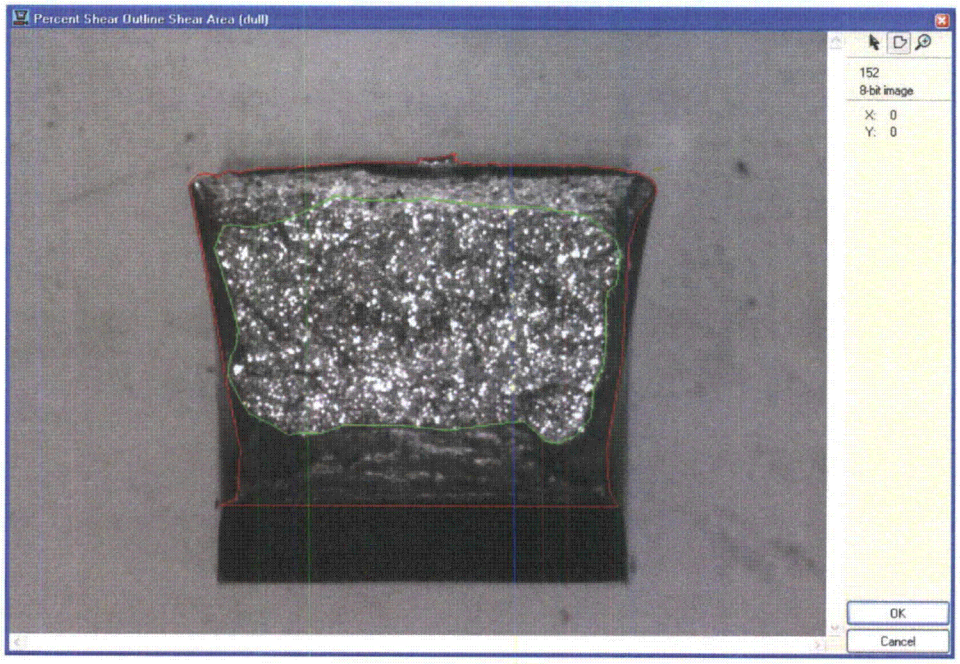

Figure 4-1
Illustration of Digital Optical Comparator Measurement of Shear Fracture Area

First, the Brittle Fracture Area is Outlined (within green line). Next, the Outer Ductile Fracture Area is Outlined (within red line). Finally, the Software Integrates the Areas and Calculates the Percent Shear Fracture Area.

4.2 Charpy Test Data for 120° Capsule

A total of eight irradiated base, weld, and HAZ metal specimens, respectively, were tested over the transition region temperature range and on the upper shelf. The data are summarized in Tables 4-1 through 4-3. In addition to the energy absorbed by the specimen during impact, the measured lateral expansion values

and the percentage shear fracture area for each test specimen are listed in the tables. The Charpy energy was acquired from the optical encoder and has been corrected for windage and friction in accordance with ASTM E23. The impact energy is the energy required to initiate and propagate a crack in the Charpy specimen. The optical encoder and the dial cannot correct for tossing energy or losses in the test machine, and therefore this small amount of additional energy, if present, may be included in the data for some tests. The instrumented striker energy does not include tossing energy or machine vibration energy since the energy, in this case, is measured only during a few milliseconds of contact between the striker and specimen. Based on comparison between the instrumented striker energy and the optical encoder energy, it has been shown that the tossing energy, and other losses, are small for most tests.

The lateral expansion is a measure of the transverse plastic deformation produced by the contact edge of the striker during the impact event. Lateral expansion is determined by measuring the maximum change of specimen thickness along the sides of the specimen. Lateral expansion is a measure of the ductility of the specimen. The nuclear industry tracks the embrittlement shift using the 35 mil (0.89 mm) lateral expansion index. In accordance with ASTM E23, the lateral expansion for some specimens, which could be broken after the impact test, should not be reported as broken since the lateral expansion of the unbroken specimen is less than that for the broken specimen. Therefore, when these conditions exist, the value listed is the unbroken measurement and a footnote is included to identify these specimens. All of the 120° capsule specimens that did not separate during the test could be broken by hand under the ASTM E23 requirements.

The percentage of shear fracture area is a direct quantification of the transition in the fracture modes as the temperature increases. All metals with a body centered cubic lattice structure, such as ferritic pressure vessel materials, undergo a transition in fracture modes. At low test temperatures, a crack propagates in a brittle manner and cleaves across the grains. As the temperature increases, the percentage of shear (or ductile) fracture increases. This temperature range is referred to as the transition region and the fracture process is mixed mode. As the temperature increases further, the fracture process is eventually completely ductile (i.e., no brittle component) and this temperature range is referred to as the upper shelf region.

Table 4-1
Irradiated Charpy V-Notch Impact Test Results for Surveillance Base Metal Specimens (Heat C2433-1) from the Susquehanna Unit 1 120° Surveillance Capsule

Base Irradiated 120° Capsule							
Specimen ID	Test Temperature		Impact Energy		Lateral Expansion		Percent Shear (%)
	°F	(°C)	ft-lb	(J)	mils	(mm)	
G4-P1-5	-100.5	(-73.6)	2.79	(3.78)	3.5	(0.09)	0.4
G4-P1-6	-44.0	(-42.2)	6.14	(8.32)	3.0	(0.08)	4.6
G4-P1-8	-0.8	(-18.2)	11.69	(15.85)	12.0	(0.30)	17.4
G4-P1-7	20.3	(-6.5)	36.9	(50.03)	32.5	(0.83)	19.8
G4-P1-1	66.4	(19.1)	60.54	(82.08)	51.0	(1.30)	27.4
G4-P1-4	108.9	(42.7)	80.43	(109.05)	61.5	(1.56)	47.7
G4-P1-2	151.7	(66.5)	118.07	(160.08)	86.5	(2.20)	100.0
G4-P1-3	302.0	(150.0)	125.73	(170.46)	88.0	(2.24)	100.0

Table 4-2
Irradiated Charpy V-Notch Impact Test Results for Surveillance Weld Metal Specimens (Heats 402K9171, 411L3071) from the Susquehanna Unit 1 120° Surveillance Capsule

Weld Irradiated 120° Capsule							
Specimen ID	Test Temperature		Impact Energy		Lateral Expansion		Percent Shear (%)
	°F	(°C)	ft-lb	(J)	mils	(mm)	
G5-P2-9	-101.9	(-74.4)	4.88	(6.62)	7.5	(0.19)	7.1
G5-P2-10	-51.0	(-46.1)	7.12	(9.65)	6.0	(0.15)	9.0
G5-P2-11	-3.1	(-19.5)	32.99	(44.73)	31.5	(0.80)	22.8
G5-P2-12	37.0	(2.8)	39.35	(53.35)	34.0	(0.86)	34.8
G4-P2-9	66.3	(19.1)	80.15	(108.67)	66.0	(1.68)	73.6
G4-P2-12	117.3	(47.4)	90.76	(123.05)	69.0	(1.75)	84.9
G4-P2-10	178.0	(81.1)	112.70	(152.80)	85.5	(2.17)	100.0
G4-P2-11	303.8	(151.0)	126.73	(171.82)	89.5	(2.27)	100.0

Table 4-3
Irradiated Charpy V-Notch Impact Test Results for Surveillance HAZ Metal Specimens from the Susquehanna Unit 1 120° Surveillance Capsule

HAZ Irradiated 120° Capsule							
Specimen ID	Test Temperature		Impact Energy		Lateral Expansion		Percent Shear (%)
	°F	(°C)	ft-lb	(J)	mils	(mm)	
G5-P3-8	-102.5	(-74.7)	6.98	(9.46)	6.0	(0.15)	7.1
G5-P3-5	-51.5	(-46.4)	8.65	(11.73)	9.5	(0.24)	13.2
G5-P3-7	-22.0	(-30.0)	59.02	(80.02)	47.0	(1.19)	32.0
G5-P3-6	1.2	(-17.1)	45.81	(62.11)	39.0	(0.99)	43.8
G5-P3-1	67.6	(19.8)	56.99	(77.27)	55.5	(1.41)	45.1
G5-P3-2	100.4	(38.0)	76.20	(103.31)	66.0	(1.68)	60.2
G5-P3-4	146.5	(63.6)	109.86	(148.95)	74.0	(1.88)	100.0
G5-P3-3	302.9	(150.5)	117.90	(159.85)	87.0	(2.21)	100.0

Section 5: Charpy Test Results

5.1 Analysis of Impact Test Results

For analysis of the Charpy test data, the BWRVIP ISP has selected the hyperbolic tangent (tanh) function as the statistical curve-fit tool to model the transition temperature toughness data. A hyperbolic tangent curve-fitting program named CVGRAPH [9] was used to fit the Charpy V-notch energy and lateral expansion data. Analysis methodology (e.g., definition of upper fixed shelf and lower shelf) followed the BWRVIP conventions established for analysis of all ISP data [20, 21]. The impact energy curve-fits from CVGRAPH are provided in Figures 5-1 (plate C2433-1) and 5-2 (weld 402K9171, 411L3071), and the lateral expansion curve-fits are shown in Figures 5-3 (plate C2433-1) and 5-4 (weld 402K9171, 411L3071). Because HAZ results are not used in the BWRVIP ISP, the HAZ data were not fit.

For the analysis of Charpy energy test data, lower shelf energy was fixed at 2.5 ft-lbs (3.4 J). Upper shelf energy was fixed at the average of all test energies exhibiting shear greater than or equal to 95%, consistent with ASTM Standard E185-82 [3]. For analysis of the lateral expansion test data, the lower shelf was fixed at 1.0 mils; the fixed upper shelf was defined as the average of the lateral expansion test data points at the same test temperatures used to define the fixed upper shelf energy.

5.2 Irradiated Versus Unirradiated CVN Properties

Table 5-1 summarizes the T_{30} [30 ft-lb (41 J) Transition Temperature], T_{35mil} [35 mil (0.89 mm) Lateral Expansion Temperature], T_{50} [50 ft-lb (68 J) Transition Temperature], and Upper Shelf Energy for the unirradiated and irradiated materials and shows the change (shift) from baseline values. The unirradiated values of T_{30} and T_{50} were taken from the CVGRAPH fits provided in Figures 2-4 and 2-5; the unirradiated values of T_{35mil} were previously determined in [20, 21]. The irradiated values are from the index temperatures determined in Figures 5-1 through 5-4.

Table 5-2 provides a comparison of the measured shifts to predicted shifts for plate heat C2433-1 and weld heat 402K9171, 411L3071. Predicted shift is based on the formula provided in Reg. Guide 1.99 Rev. 2 [6] as shown in Note 2 to Table 5-2. The fluence was input as 5.75×10^{17} n/cm^2, as reported in Table 3-8 for the 120° capsule. For surveillance plate heat C2433-1, the measured shift is within the value expected (e.g., the measured shift is less than predicted

shift + margin); however, the measured shift for weld heat 402K9171, 411L3071 is about 2.5 times greater than the predicted shift + margin.

Measured percent decrease in USE is presented in Table 5-3 and compared to the percent decrease predicted by Figure 2 of Reg. Guide 1.99, Rev. 2. For both the surveillance plate and weld, the measured percent decrease is less than the predicted percent decrease.

Irradiated Plate Heat C2433-1 (SH1-120)

CVGRAPH 5.0.2 Hyperbolic Tangent Curve Printed on 12/22/2012 05:16 PM
Page 1
Coefficients of Curve 1
A = 62.2 B = 59.7 C = 77.08 T0 = 70.51 D = 0.00E+00
Equation is A + B * [Tanh((T-To)/(C+DT))]
Upper Shelf Energy=121.9(Fixed) Lower Shelf Energy=2.5(Fixed)
Temp@30 ft-lbs=24.1 Deg F Temp@50 ft-lbs=54.6 Deg F
Plant: Susquehanna 1 Material: SA533B1 Heat: C2433-1
Orientation: LT Capsule: 120 de Fluence: n/cm^2

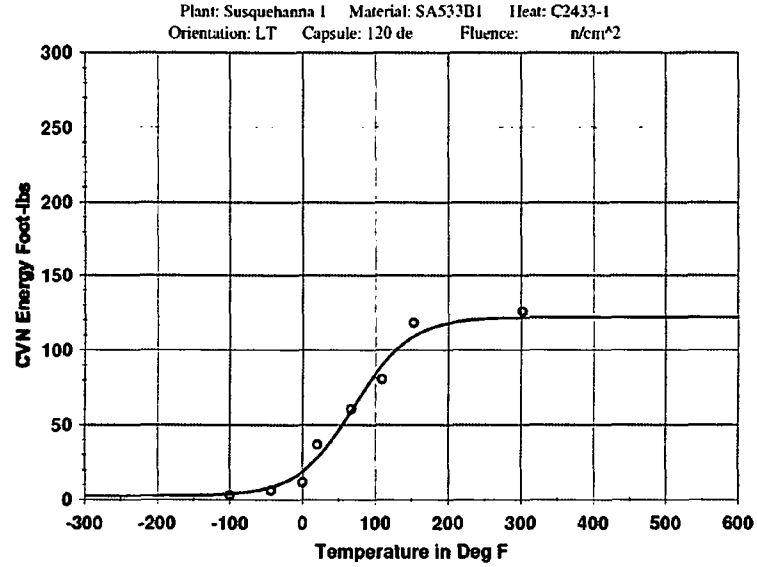

Charpy V-Notch Data

Temperature	Input CVN	Computed CVN	Differential
-100.50	2.79	3.90	-1.11
-44.00	6.14	8.32	-2.18
-.80	11.69	18.72	-7.03
20.30	36.90	28.02	8.88
66.40	60.54	59.02	1.52
108.90	80.43	89.69	-9.26
151.70	118.07	108.95	9.12
302.00	125.73	121.61	4.12

Correlation Coefficient = .991

Figure 5-1
Irradiated Plate C2433-1 Charpy Energy Plot (Susquehanna Unit 1 120° Capsule)

Irradiated Weld Heat 402K9171/411L3071 (SH1-120)

CVGRAPH 5.0.2 Hyperbolic Tangent Curve Printed on 12/22/2012 05:22 PM
Page 1
Coefficients of Curve 1
A = 61.11 B = 58.61 C = 87.15 T0 = 54.78 D = 0.00E+00
Equation is A + B * [Tanh((T-To)/(C+DT))]
Upper Shelf Energy=119.7(Fixed) Lower Shelf Energy=2.5(Fixed)
Temp@30 ft-lbs=3.3 Deg F Temp@50 ft-lbs=38.1 Deg F
Plant: Susquehanna 1 Material: SMAW Heat: 402K9171/411
Orientation: NA Capsule: 120 de Fluence: n/cm^2

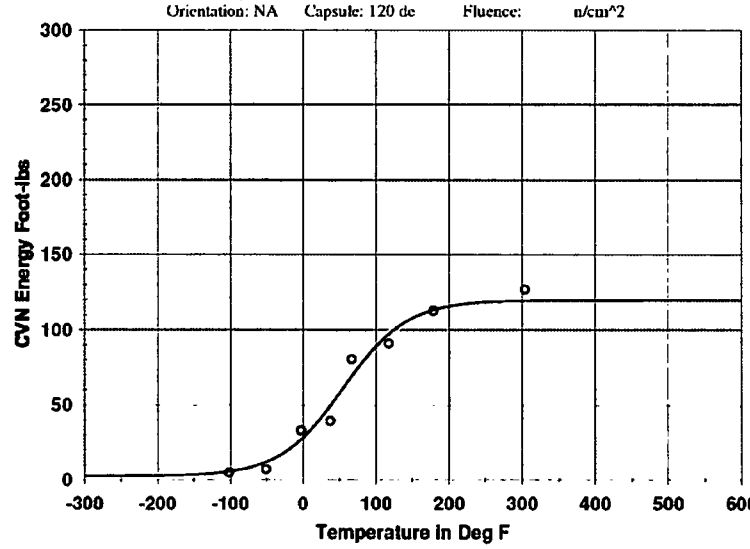

Charpy V-Notch Data

Temperature	Input CVN	Computed CVN	Differential
-101.90	4.88	5.63	-.75
-51.00	7.12	12.01	-4.89
-3.10	32.99	27.05	5.94
37.00	39.35	49.31	-9.96
66.30	80.15	68.81	11.34
117.30	90.76	97.17	-6.41
178.00	112.70	113.17	-.47
303.80	126.73	119.33	7.40

Correlation Coefficient = .988

Figure 5-2
Irradiated Weld Heat 402K9171, 411L3071 Charpy Energy Plot (Susquehanna Unit 1 120° Capsule)

Irradiated Plate Heat C2433-1 LE (SH1-120)

CVGRAPH 5.0.2 Hyperbolic Tangent Curve Printed on 12/22/2012 05:19 PM
Page 1
Coefficients of Curve 1
A = 44.13 B = 43.13 C = 78.43 T0 = 56.79 D = 0.00E+00
Equation is A + B * [Tanh((T-To)/(C+DT))]
Upper Shelf L.E.=87.3(Fixed) Lower Shelf L.E.=1.0(Fixed)
Temp.@L.E. 35 mils=40.0 Deg F
Plant: Susquehanna 1 Material: SA533B1 Heat: C2433-1
Orientation: LT Capsule: 120 de Fluence: n/cm^2

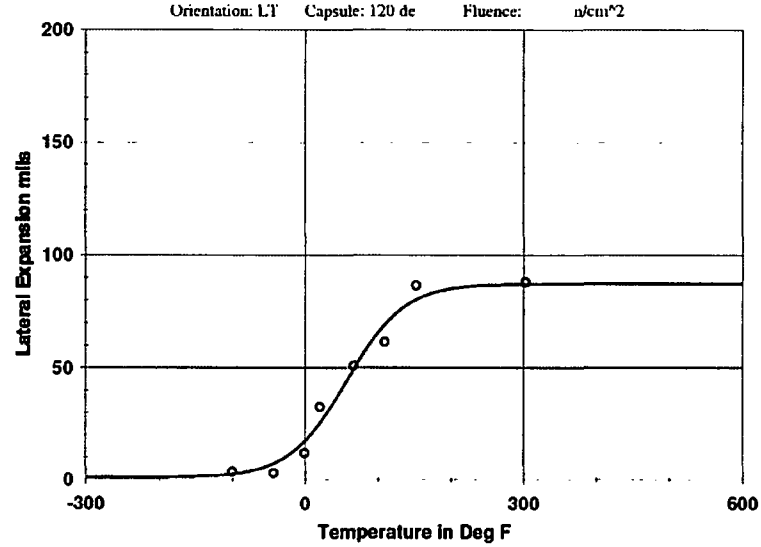

Charpy V-Notch Data

Temperature	Input L.E.	Computed L.E.	Differential
-100.50	3.50	2.54	.96
-44.00	3.00	7.13	-4.13
-.80	12.00	17.14	-5.14
20.30	32.50	25.40	7.10
66.40	51.00	49.39	1.61
108.90	61.50	69.19	-7.69
151.70	86.50	80.21	6.29
302.00	88.00	87.08	.92

Correlation Coefficient = .989

Figure 5-3
Irradiated Plate C2433-1 Lateral Expansion Plot (Susquehanna Unit 1 120° Capsule)

Irradiated Weld 402K9171/411L3071 LE (SH1-120)

CVGRAPH 5.0.2 Hyperbolic Tangent Curve Printed on 12/22/2012 05:24 PM
Page 1
Coefficients of Curve 1
A = 44.25 B = 43.25 C = 90.16 T0 = 39.26 D = 0.00E+00
Equation is A + B * [Tanh((T-To)/(C+DT))]
Upper Shelf L.E.=87.5(Fixed) Lower Shelf L.E.=1.0(Fixed)
Temp.@L.E. 35 mils=19.7 Deg F
Plant: Susquehanna 1 Material: SMAW Heat: 402K9171/411
Orientation: NA Capsule: 120 de Fluence: n/cm^2

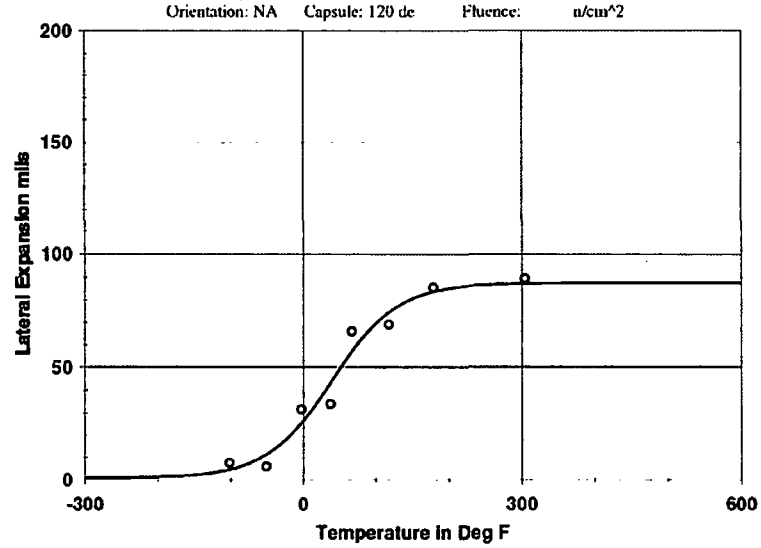

Charpy V-Notch Data

Temperature	Input L.E.	Computed L.E.	Differential
-101.90	7.50	4.62	2.88
-51.00	6.00	11.29	-5.29
-3.10	31.50	25.30	6.20
37.00	34.00	43.16	-9.16
66.30	66.00	56.84	9.16
117.30	69.00	74.49	-5.49
178.00	85.50	83.69	1.81
303.80	89.50	87.26	2.24

Correlation Coefficient = .982

Figure 5-4
Irradiated Weld Heat 402K9171, 411L3071 Lateral Expansion Plot (Susquehanna Unit 1 120° Capsule)

Table 5-1
Effect of Irradiation (E>1.0 MeV) on the Notch Toughness Properties

Material Identity	T_{30}, 30 ft-lb (40.7 J) Transition Temperature			T_{50}, 50 ft-lb (67.8 J) Transition Temperature			T_{35mil}, 35 mil (0.89 mm) Lateral Expansion Temperature			CVN Upper Shelf Energy (USE)		
	Unirrad °F (°C)	Irradiated °F (°C)	ΔT_{30} °F (°C)	Unirrad °F (°C)	Irradiated °F (°C)	ΔT_{50} °F (°C)	Unirrad °F (°C)	Irradiated °F (°C)	ΔT_{35mil} °F (°C)	Unirrad ft-lb (J)	Irradiated ft-lb (J)	Change ft-lb (J)
C2433-1 (LT orientation)	8.1 (-13.3)	24.1 (-4.4)	16.0 (8.9)	35.4 (1.9)	54.6 (12.6)	19.2 (10.7)	19.7 (-6.8)	40.0 (4.4)	20.3 (11.3)	130.3 (176.7)	121.9 (165.3)	-8.4 (-11.4)
402K9171, 411L3071	-39.6 (-39.8)	3.3 (-15.9)	42.9 (23.8)	2.2 (-16.6)	38.1 (3.4)	35.9 (19.9)	-9.4 (-23.0)	19.7 (-6.8)	29.1 (16.2)	107.7 (146.0)	119.7 (162.3)	12.0 (16.3)

Table 5-2
Comparison of Actual Versus Predicted Embrittlement

Identity	Material	Fluence ($\times 10^{17}$ n/cm^2)	Measured Shift[1] °F (°C)	RG 1.99 Rev. 2 Predicted Shift[2] °F (°C)	RG 1.99 Rev. 2 Predicted Shift+Margin[2,3] °F (°C)
C2433-1 (LT orientation)	Susquehanna Unit 1 surveillance plate	5.75	16.0 (8.9)	20.56 (11.4)	41.1 (22.8)
402K9171, 411L3071	Susquehanna Unit 1 surveillance weld	5.75	**42.9 (23.8)**	8.5 (4.7)	17.0 (9.5)

1. The measured shift is taken from Table 5-1.
2. Predicted shift = CF × FF, where CF is a Chemistry Factor taken from tables from USNRC RG 1.99, Rev. 2 [6], based on each material's Cu/Ni content, and FF is Fluence Factor, $f^{0.28-0.10 \log f}$, where f = fluence in units of 10^{19} n/cm^2 (E > 1.0 MeV) specified.
3. Margin = $2\sqrt{(\sigma_i^2 + \sigma\Delta^2)}$, where σ_i = the standard deviation on initial RT_{NDT} (which is taken to be 0°F), and $\sigma\Delta$ is the standard deviation on ΔRT_{NDT} (28°F for welds and 17°F for base materials, except that $\sigma\Delta$ need not exceed 0.50 times the mean value of ΔRT_{NDT}). Thus, margin is defined as 34°F for plate materials and 56°F for weld materials, or margin equals shift (whichever is less), per Reg. Guide 1.99, Rev. 2.

Table 5-3
Percent Decrease In Upper Shelf Energy

Identity	Material	Capsule	Fluence ($x10^{17}$ n/cm^2)	Measured Decrease in USE[1] (%)	Predicted Decrease in USE[2] (%)
C2433-1 (LT orientation)	Susquehanna Unit 1 surveillance plate	120°	5.75	6.45	9.7
402K9171, 411L3071	Susquehanna Unit 1 surveillance weld	120°	5.75	-11.14	8.1

1. Calculated from Table 5-1, (Change/Unirradiated) * 100. A positive number indicates a decrease in USE; a negative number indicates the USE increased over the unirradiated value.
2. Based on the equations of Figure 2 of Reg. Guide 1.99 Rev. 2 [6] as provided in Reg. Guide 1.162 [22].

Section 6: References

1. 10 CFR 50, Appendices G (*Fracture Toughness Requirements*) and H (*Reactor Vessel Material Surveillance Program Requirements*), Federal Register, Volume 60, No. 243, dated December 19, 1995.
2. American Society of Mechanical Engineers (ASME) Boiler and Pressure Vessel Code (Code), Section XI, "Rules for In service Inspection of Nuclear Power Plant Components," Nonmandatory Appendix G, Fracture Toughness Criteria for Protection Against Failure.
3. ASTM E185-82, *Standard Practice for Conducting Surveillance Tests for Light-Water Cooled Nuclear Power Reactor Vessels*, E706 (IF), ASTM Standards, Section 3, American Society for Testing and Materials, Philadelphia, PA, 1993.
4. *BWRVIP-86, Revision 1-A: BWR Vessel and Internals Project, Updated BWR Integrated Surveillance Program (ISP) Implementation Plan.* EPRI, Palo Alto, CA: 2012. 1025144.
5. 10 CFR 50, Appendix B, "Quality Assurance Criteria for Nuclear Power Plants and Fuel Reprocessing Plants."
6. U.S. NRC Regulatory Guide 1.99, "Radiation Embrittlement of Reactor Vessel Materials," Revision 2, May 1988.
7. "Guidelines for the Management of Materials Issues," NEI 03-08, Nuclear Energy Institute, Washington, DC, Latest Edition.
8. "Susquehanna Steam Electric Station Unit 1 Vessel Surveillance Materials Testing and Fracture Toughness Analysis", R.G. Carey, GE Nuclear Energy, GE-NE-523-169-1292, Revision 1, October, 1993.
9. CVGRAPH, Hyperbolic Tangent Curve Fitting Program, Developed by EPRI, Version 5.0.2, Revision 1, 3/26/02.
10. "Calculational and Dosimetry Methods for Determining Pressure Vessel Neutron Fluence," Nuclear Regulatory Commission Regulatory Guide 1.190, March 2001.
11. *BWRVIP-126: BWR Vessel Internals Project, RAMA Fluence Methodology Software*, Version 1.0. EPRI, Palo Alto, CA: 2003. 1007823.
12. Letter from William H. Bateman (U.S. NRC) to Bill Eaton (BWRVIP), Safety Evaluation of Proprietary EPRI Reports BWRVIP-114, -115, -117, and -121 and TWE-PSE-001-R-001. dated May 13, 2005.

13. Letter from Matthew A. Mitchell (U.S. NRC) to Rick Libra (BWRVIP), "Safety Evaluation of Proprietary EPRI Report BWR Vessel and Internals Project, Evaluation of Susquehanna Unit 2 Top Guide and Core Shroud Material Samples Using RAMA Fluence Methodology (BWRVIP-145)," dated February 7, 2008.

14. *"BUGLE-96: Coupled 47 Neutron, 20 Gamma-Ray Group Cross Section Library Derived from ENDF/B-VI for LWR Shielding* and Pressure Vessel Dosimetry Applications," RSICC Data Library Collection, DL2C-185, March 1996.

15. "VITAMIN-B6: A Fine-Group Cross Section Library Based on ENDF/B-VI Release 3 for Radiation Transport Applications," RSICC Data Library Collection, DL2C-184, December 1996.

16. *BWRVIP-114-A: BWR Vessel and Internals Project, RAMA Fluence Methodology Theory Manual*, EPRI, Palo Alto, CA: 2009. 1019049.

17. *BWRVIP-121-A: BWR Vessel and Internals Project, RAMA Fluence Methodology Procedures Manual*, EPRI, Palo Alto, CA: 2009. 1019052.

18. P. K. Nair, E. B. Norris, M. L. Williams, *Susquehanna Unit 1 Dosimeter Testing*, Southwest Research Institute, Project No. 06-8658, September 1986.

19. ASTM Standard E23, 2002, "Standard Test Methods for Notch Bar Impact Testing of Metallic Materials," ASTM International, West Conshohocken, PA, 2002, DOI: 10.1520/E0023-02, www.astm.org.

20. *BWRVIP-135, Revision 2: BWR Vessel and Internals Project, Integrated Surveillance Program (ISP) Data Source Book and Plant Evaluations.* EPRI, Palo Alto, CA: 2009. 1020231.

21. BWRVIP Letter 2010-238, Errata for BWRVIP-135, Rev. 2, October 15, 2010.

22. U.S. NRC Regulatory Guide 1.162, "Format and Content of Report for Thermal Annealing of Reactor Pressure Vessels," February 1996.

Appendix A: Dosimeter Analysis

A.1 Dosimeter Material Description

The Susquehanna 1 120° surveillance capsule primary dosimeter materials are pure metal wires which were located within the surveillance capsule Charpy packets. The wire types provided for the Susquehanna 1 surveillance program are copper, iron, and nickel. Each wire is about three inches (7.62 cm) long with one of each type included in the two Charpy specimen packets.

A.2 Dosimeter Cleaning and Mass Measurement

At the time the Charpy packets were opened, the dosimeter wires were cleaned in an ultrasonic cleaner and wiped with acetone wetted wipes to remove loose contamination. Upon receipt at the radiometric lab, the wires were visually inspected under a low magnification optical microscope. There was evidence of oxidation indicating the need for chemical etching and further cleaning. This was accomplished by soaking the Fe wire segments in a 4N solution of hydrochloric acid until the oxidation was etched from the surface. Similarly, the Ni and Cu wires were immersed in a 2N solution of nitric acid solution. The wires were then rinsed with distilled water, wiped once more with ethanol, and then allowed to dry in air at room temperature. The wires then exhibited a clean, shiny appearance. Figures A-1 through A-6 show low-power magnifications of the dosimetry wires as they were found prior to cleaning, and after cleaning and coiling. In general, the iron and copper wires had experienced the most oxidation, while the nickel wires were relatively clean at the time of recovery from the Charpy packets.

The total mass of each wire was measured using a Mettler Toledo XS105DU analytical digital balance. Table A-1 lists the results of these measurements, as well as the identification assigned to each dosimeter. The dosimeters identifications were assigned as the Charpy packet numbers followed by the type of dosimeter material.

As previously mentioned, the wires were tightly coiled for subsequent counting and weighing. Each wire was wrapped around a thin metal rod to form a coil of approximately 0.5 inch (12.7 mm) diameter or less, which yields a reasonable approximation to a point source geometry at the distance the dosimeter wires are placed from the gamma detector. The coiled wire segments were pressed firmly against a hard surface to flatten the coil to yield the best counting geometry.

A.3 Radiometric Analysis

Radiometric analysis was performed using high resolution gamma emission spectroscopy. In this method, gamma emissions from the dosimeter materials are detected and quantified using solid-state gamma ray detectors and computer-based signal processing and spectrum analysis. The specifications of the gamma ray spectrometer system (GRSS) are listed in Table A-2. The GRSS features a hyper pure germanium (HPGe) detector that is housed in a lead-copper shield to reduce background count rates. Standard background subtraction procedures were used.

GRSS calibration was performed using a National Institute for Standards and Technology (NIST) traceable mixed gamma quasi-point source. The Canberra analysis software provides the capability for energy resolution and efficiency calibration using specified standard source information. Calibration information is stored on magnetic disk for use by the spectrographic analysis software package.

Since detector efficiency depends on the source-detector geometry, a fixed-reproducible geometry must be selected for the gamma spectrographic analysis of the dosimeter materials. For the dosimeter wires, the counting geometry was that of a quasi-point source (coiled wire) placed five inches (12.7 cm) vertically from the top surface of the detector shell. In this way, extended sources up to 0.5 inch (1.27 cm) can be analyzed with a good approximation to a point source. The coiled wires were well within the area needed to approximate a point source geometry. The HPGe detector was calibrated for efficiency using the NIST traceable source. The accuracy of the efficiency calibration was checked using a gamma spectrographic analysis of the NIST traceable mixed gamma source. The isotopes contained in the source emit gamma rays which span the energy response of the detector for the dosimeter materials. These measurements show that the efficiency calibration is providing a valid measurement of source activity. The acceptance criteria for these measurements are that the software must yield a valid isotopic identification, and that the quantified activity of each correctly identified isotope must be within the uncertainty specified in the source certification. Validation of system performance was made prior to starting the counting tasks, and upon completion of all counting work for Susquehanna 1. The counting system performance was acceptable in each case, indicating that the counting system properties did not change during the course of the counting procedure.

Table A-3 shows the counting schedule established for this work. There was no requirement for order of counting since the dosimeter materials still contained sufficient quantities of activation products to allow accurate radio assay. Counting times were more than sufficient to achieve the desired statistical accuracy for gamma emissions of interest in all cases.

Neutrons interact with the constituent nuclei of the dosimeter materials producing radionuclides in varying amounts depending on total neutron fluence, its energy spectrum, and the nuclear properties of the dosimeter materials. Table

A-4 lists the reactions of interest and their resultant radionuclide products for each element contained in the dosimeters. These are threshold reactions involving an n-p or n-α interaction.

Finally, Table A-5 presents the primary results of interest for flux and fluence determination.
The specific activity units are in dps/mg, which normalizes the activity to dosimeter mass. The activities are specified for a useful reference date/time, which in this case is the Susquehanna 1 plant shutdown date and time. This reference date/time was specified as March 31, 2012, at 1:33:00 AM eastern standard time.

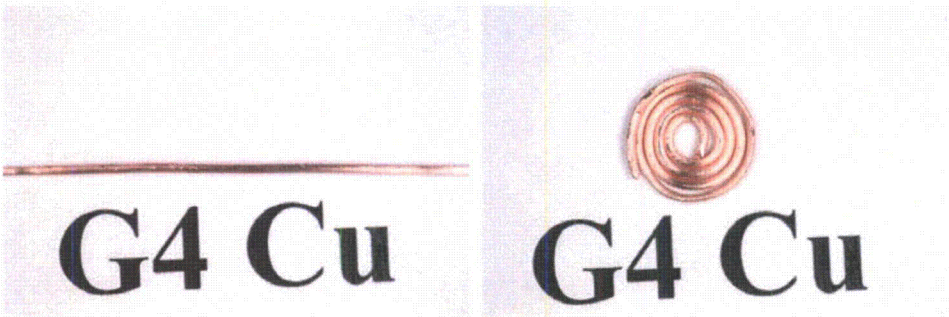

Figure A-1
Charpy Packet G4 Cu Dosimeter Wire: Prior to Cleaning (left); and After Cleaing/Coiling (right)

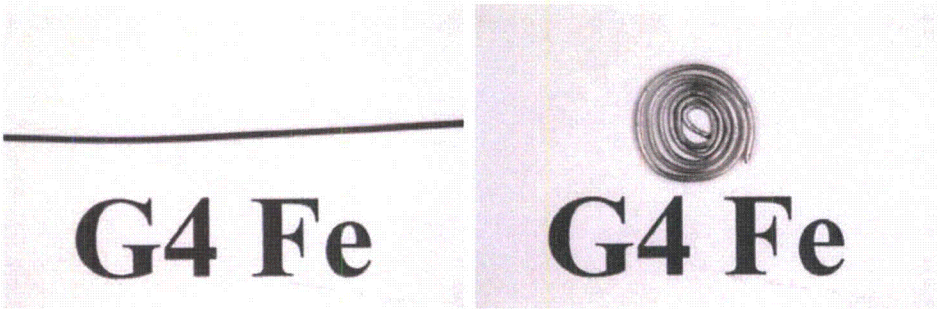

Figure A-2
Charpy Packet G4 Fe Dosimeter Wire: Prior to Cleaning (left); and After Cleaning/Coiling (right)

Figure A-3
Charpy Packet G4 Ni Dosimeter Wire: Prior to Cleaning (left); and After Cleaning/Coiling (right)

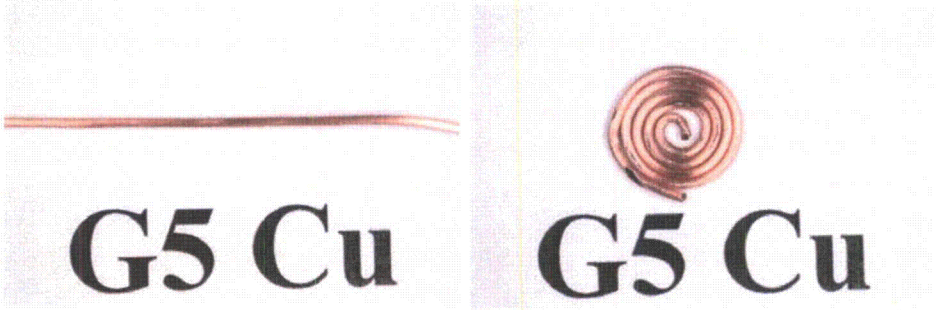

Figure A-4
Charpy Packet G5 Cu Dosimeter Wire: Prior to Cleaning (left); and After Cleaing/Coiling (right)

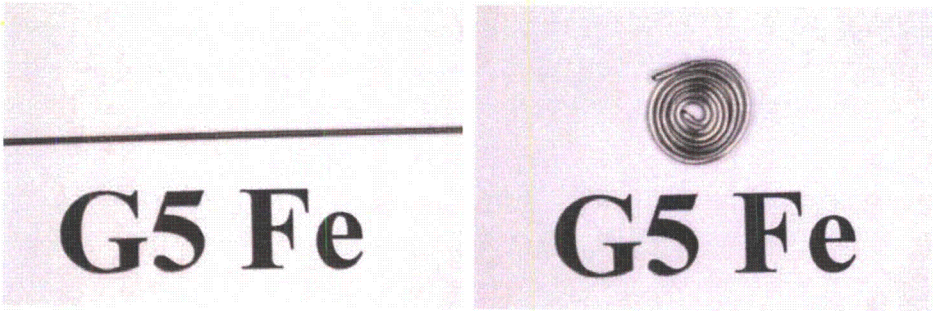

Figure A-5
Charpy Packet G5 Fe Dosimeter Wire: Prior to Cleaning (left); and After Cleaning/Coiling (right)

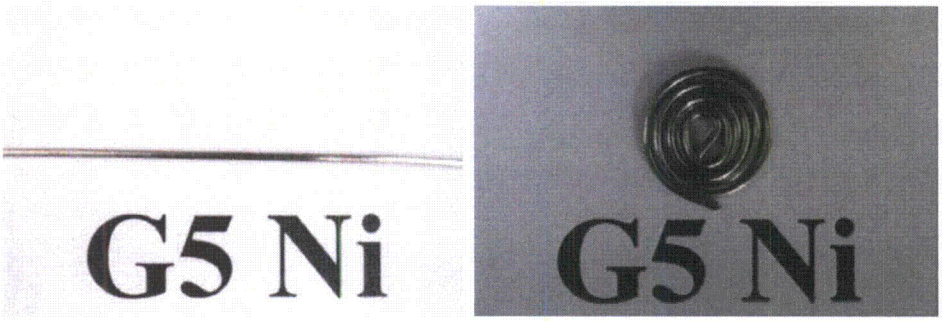

Figure A-6
Charpy Packet G5 Ni Dosimeter Wire: Prior to Cleaning (left); and After Cleaning/Coiling (right)

Table A-1
Susquehanna 1 120° Capsule Charpy Packet Dosimeter Wire Masses

Wire Dosimeter ID	Mass (mg)
G4 Cu	319.10
G4 Fe	148.86
G4 Ni	306.62
G5 Cu	355.65
G5 Fe	152.06
G5 Ni	311.94

Table A-2
Gamma Ray Spectrometer System (GRSS) Specifications

System Component	Description and/or Specifications
Detector	Canberra Model GC1518
Energy Resolution	1.8keV @ 1.33 MeV
Detector Efficiency Relative to a 3 inch x 3 inch NaI Crystal	15% at 1.3 MeV
Amplifier/Multichannel Analyzer	Canberra DAS-1000
Computer System	Intel i5-2500 CPU at 3.30 GHz,, 2.91 GB Main Memory, 931 GB Hard Disk, 17-inch Monitor, HP LaserJet Printer
Software	Canberra Apex v 1.2

Table A-3
Counting Schedule for Susquehanna 1 120° Capsule Dosimeter Materials

Dosimeter ID	Count Start Date	Count Start Time (EST)	Count Duration (Live Time Seconds)
G4 Cu	11/08/12	3:33 PM	86,400
G4 Fe	11/07/12	3:08 PM	86,400
G4 Ni	11/15/12	11:04 AM	86,400
G5 Cu	11/17/12	12:05 AM	86,400
G5 Fe	11/16/12	11:45 AM	86,400
G5 Ni	11/19/12	7:44 AM	86,400

Table A-4
Neutron-Induced Reactions of Interest

Dosimeter Material	Neutron-Induced Reaction	Reaction Product Radionuclide
Iron	$^{54}Fe(n,p)^{54}Mn$	^{54}Mn
Copper	$^{63}Cu(n, \alpha)^{60}Co$	^{60}Co
Nickel	$^{58}Ni(n.p)^{58}Co$	^{58}Co

Table A-5
Results of Susquehanna 1 120° Capsule Radiometric Analysis

Dosimeter ID	Isotope ID	Activity at Reference Date/Time[a] (µCi)	Specific Activity at Reference Date/Time[a] (dps/mg)	Activity Uncertainty (%)
G4 Cu	^{60}Co	1.05E-01	12.17	1.89
G4 Fe	^{54}Mn	2.82E-01	70.09	2.56
G4 Ni	^{58}Co	9.43E+00	1137.91	2.65
G5 Cu	^{60}Co	1.26E-01	13.11	1.89
G5 Fe	^{54}Mn	3.19E-01	77.62	2.56
G5 Ni	^{58}Co	9.18E+00	1088.86	2.65

[a] March 31, 2012 at 1:33:00 AM EST is the reference date and time.

The Electric Power Research Institute, Inc. (EPRI, www.epri.com) conducts research and development relating to the generation, delivery and use of electricity for the benefit of the public. An independent, nonprofit organization, EPRI brings together its scientists and engineers as well as experts from academia and industry to help address challenges in electricity, including reliability, efficiency, affordability, health, safety and the environment. EPRI also provides technology, policy and economic analyses to drive long-range research and development planning, and supports research in emerging technologies. EPRI's members represent approximately 90 percent of the electricity generated and delivered in the United States, and international participation extends to more than 30 countries. EPRI's principal offices and laboratories are located in Palo Alto, Calif.; Charlotte, N.C.; Knoxville, Tenn.; and Lenox, Mass.

Together...Shaping the Future of Electricity

Program:

Nuclear Power

BWR Vessel and Internals Project

3002000685

Electric Power Research Institute
3420 Hillview Avenue, Palo Alto, California 94304-1338 • PO Box 10412, Palo Alto, California 94303-0813 USA
800.313.3774 • 650.855.2121 • askepri@epri.com • www.epri.com